SYNTHESIS OF PERYLENE DIIMIDES AND OLIGOTHIOPHENES AS PHOTOACTIVE MONOMERS IN COVALENT ORGANIC FRAMEWORKS

A Thesis

Presented to the Faculty of the Graduate School

of Cornell University

in Partial Fulfillment of the Requirements for the Degree of

Master of Science

by

Sonia Grace Thangavelu

May 2010

ABSTRACT

Covalent organic frameworks (COFs) are an emerging class of materials that have received remarkable attention as gas storage materials as a result of their continuous porosity, high surface area, and thermal resistivity. A review of the literature in the field reveals synthetic methodologies toward improving their gas storage capabilities by maximizing their surface area and pore size; yet their function as light-harvesting materials is relatively minimal.

In pursuit of creating organic semiconductors capable of effective electron transfer pathways, COFs may be a possible alternative to achieve this goal with respect to their high degree of structural order.

From these perspectives, the design of *n*-type perylene diimide (PDI) and *p*-type oligothiophene building blocks was developed. The synthesis of these compounds by transition-metal cross-coupling or lithiation-borylation protocols was explored, and these compounds show promising signs as potential candidates to form a new class of COF materials with photoconductive functions.

BIOGRAPHICAL SKETCH

Sonia Grace Thangavelu graduated in 2003 from Springbrook High School, Silver Spring, MD, and in 2006 from Towson University (*summa cum laude*), Baltimore, MD. At Towson, she undertook her first research endeavor under Professor Clare Muhoro, a dear friend and amazing mentor, publishing her first paper in the *Journal of Organometallic Chemistry* in 2008, and winning the ACS American Institute of Chemistry student award. The thrill and joy of making a difference in the scientific community motivated her to take a job at the Department of Defense as a laboratory technician based at Walter Reed Army Institute of Research in Washington, DC, under Dr. Richard Gordon, from 2007 to 2008. After receiving the Paul A. Siple Memorial Award, presented by the United States Army, for her paper in *Chemico-Biological Interactions*, she co-authored a patent on the novel drug design of bis(pyridinium)oximes against organophosphate nerve agents in 2009. She enrolled in Cornell University in 2008, under the supervision of her thesis advisor, Professor William Dichtel. She decided to leave Cornell with a master's degree in 2010 and is actively pursing her PhD.

To Mom, Dad, Kavita, Veena, and my best buddy, Sean.

ACKNOWLEDGMENTS

I would like to first thank my thesis advisor, Professor William Dichtel, for his support, inspiration, and, more important, his encouragement despite times of amazement and frustration in designing our compounds in the field of materials science. He is an avid instructor and extremely knowledgeable individual; much of this document could not have been written without his valuable input. I also would like to thank Professor Abruña and Professor Coates for serving on my committee; especially Professor Coates's passion and breadth for teaching new synthetic methods in polymer chemistry in my coursework. I would also like to thank my editor, Kristen Ebert-Wagner, for her help in proofreading and making this document enjoyable to read.

Professionally, I would like to thank Professor Abruña's group for CV experiments and DFT calculations, and for helping me understand the electrochemistry behind our materials. I would also like to thank Dr. Ivan Keresztes and Anthony Condo for providing access to NMR, GC-MS, and MALDI-TOF facilities through the Cornell Center for Materials Research (CCMR). I would also like to acknowledge Mr. Bob Sherwood, from the Biotechnology Building at Cornell University, for structural characterization and for suggesting appropriate MALDI matrices to design my own MALDI-TOF experiments.

Finally, I would like to thank my Fantastic Four crew—Sean Conte, Jimmy John, Hoang Le, and Laura Tomasevich. Because of them my experiences at Cornell were truly enjoyable, and our adventures together will continue for many years to come.

Most of all, I would like to thank Mom, Dad, Kavita, Veena, and Sean for all of their support, love, frequent visits to frigid Ithaca, encouragement, and, more important, their faith and determination to help me arrive where I am today. Without

them, my strong will to drive forward socially, academically, and economically in our ever-demanding society would come to nothing.

TABLE OF CONTENTS

LIST OF FIGURES

LIST OF TABLES

CHAPTER 1:

Covalent Organic Frameworks: Emerging Solid-State Organic Materials

1.1. The importance of covalent organic frameworks

Covalent organic frameworks (COFs) are crystalline polymer solids composed entirely of lightweight elements (C, O, B, N, or Si) that form strong covalent bonds, which self-assemble into porous networks from molecular building blocks via condensation reactions (Figure 1.1).

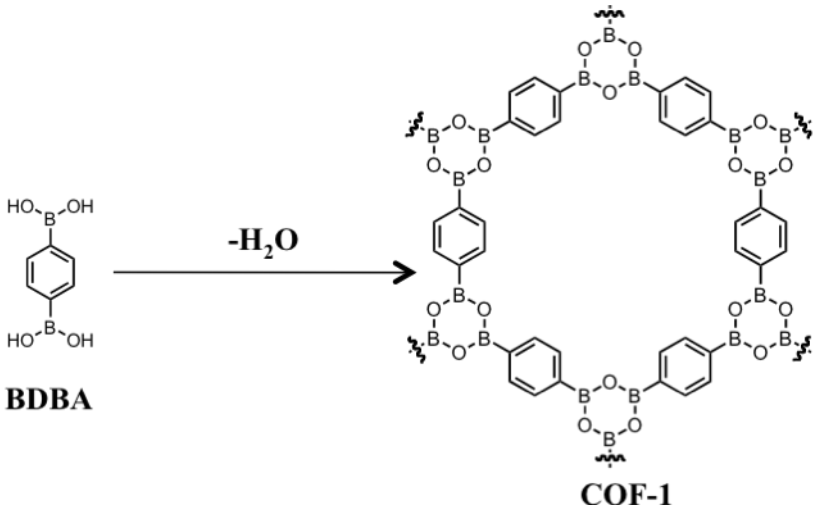

Figure 1.1. Example of a covalent organic framework using a BDBA building block.

Unlike the design of linear polymers, which tend to form random entanglements in solution, that of COFs offers considerable advantages: COFs form precise and predictable structures as two dimensional (2D) sheets or three dimensional (3D) lattices, exhibit high surface area, and demonstrate continuous porosity; and their synthesis is scalable and inexpensive. Based on these properties, COFs are attractive candidates for many environmental applications.

In the past five years, synthetic methodologies to maximize the pore size and surface area of COFs used as exceptional gas storage systems have been

demonstrated; however, their functions as potential catalytic or photonic devices have remained relatively unexplored, and there are only two cited examples of their use as photoluminescent materials[1-2]. This chapter presents a history of COFs, traces their evolution from gas storage to photonic materials, and discusses the possibility of designing new photonic COFs.

1.2. History of COFs from 2005 to 2010

1.2.1. Study of 2D boronic acid COFs as gas storage systems

Materials similar to COFs known as metal organic frameworks (MOFs), which are porous networks composed of organic ligands and metal ions, were described by several groups before the invention of COFs; however, COFs were first reported by Yaghi and colleagues in 2005. Since then, the field has grown, extending to 54 publications and including the synthesis of 20 different COFs with applications in gas storage, catalysis, and, finally, electronic materials.

The synthesis of 2D boronic acid COFs[3-6], specifically COF-1, COF-5, COF-6, COF-8, and COF-10, by Yaghi et al. is demonstrated by co-condensation of aryl diboronic acids (BDBA, BTBA, TBPA, and BPDA) with hexahydroxytriphenylene (HHTP) in dioxane: mesitylene (1:1) at 120 °C (Figure 1.2). The surface area, pore diameter, and gas uptake (H_2, CO_2, CH_4) of these COFs[3-6] were studied, and they were found to be very porous materials and to have excellent gas uptake (Table 1.1).

In 2009, Campbell and colleagues[7] demonstrated a faster and more convenient method for synthesizing COF-5 by microwave irradiation of BDBA and HHTP in dioxane: mesitylene (1:1) for 20 min at 100 °C. Interestingly, the surface area was found to be 2019 $m^2\ g^{-1}$, 1.3 times larger than the surface area of COF-5 reported by Yaghi et al[4]. The authors hypothesized that the increased surface area of COF-5

samples prepared by microwave irradiation was due to improved removal of impurities trapped in the pores.

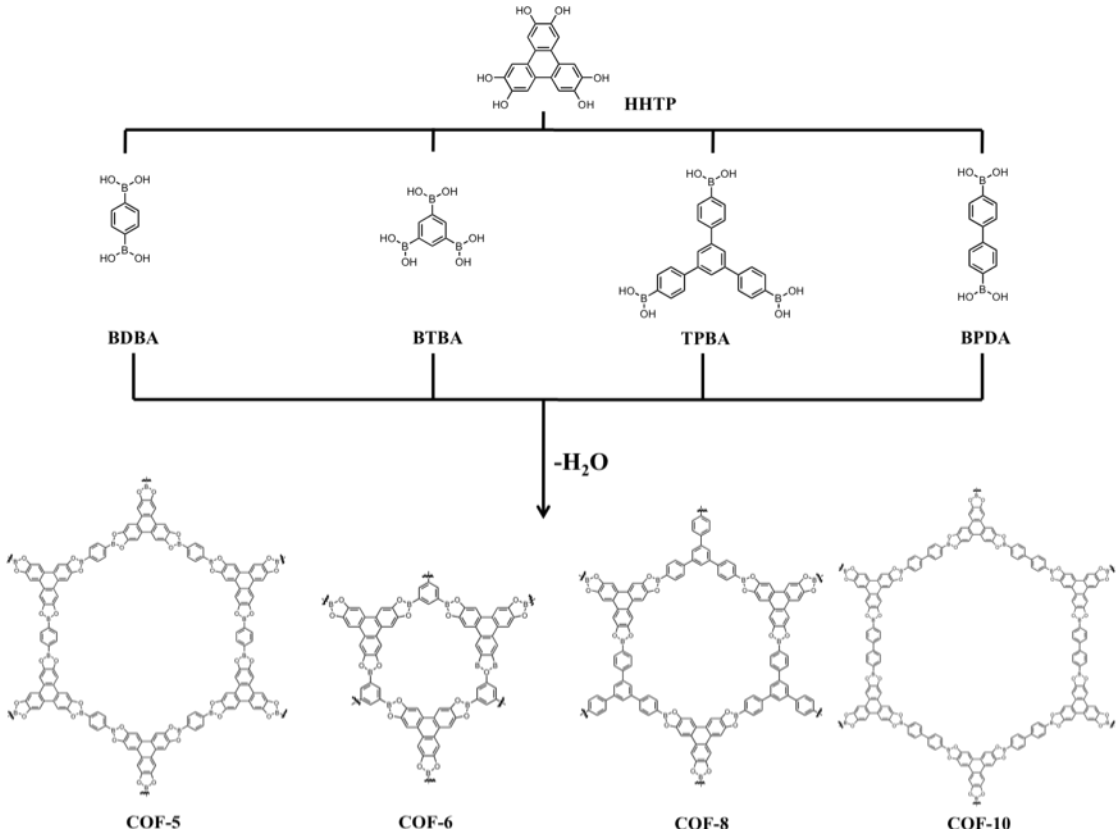

Figure 1.2. Representative 2D COFs (Furukawa, H.; Yaghi, O. *J. Am. Chem. Soc.* **2009**, *131*, 8875-8883. Copyright American Chemical Society. Reproduced with permission.).

Another representative class of COFs, created by Lavigne and colleagues[3,8-9] in 2006, involves the condensation of BTBA and dialkyl substituted 1,2,4,5-tetrahydroxybenzene (THB) to form COF-18Å, COF-16Å, COF-14Å, and COF-11Å, respectively (Figure 1.3). The surface areas of COF-18Å, COF-16Å, COF-14Å, and COF-11Å were reported to be 1260, 750, 800, and 100 m^2 g^{-1}, with upper values similar to that for COF-5. A remarkable result reported by Lavigne et al. illustrates the direct correlation of increased alkylation to pore diameter where tailoring the microporosity of COFs can be controlled for specific hydrogen uptake applications[9].

Table 1.1. Surface area, pore diameter, and gas uptake of reported 2D COFs [3-6; ‡]

Material	Pore diameter/ Å	S_{BET}/ m^2 g^{-1}	H_2 uptake/ mg g^{-1}	CH_4 uptake/ mg g^{-1}	CO_2 uptake/ mg g^{-1}
COF-1	15	711	14.8	40	230
COF-5	27	1590	35.8	89	870
COF-6	9	980	22.6	65	310
COF-8	16	1400	35.0	87	630
COF-10	32	2080	39.2	80	1010

‡ H_2 uptake is the saturation H_2 uptake at 77 K. CH_4 and CO_2 uptake are at 35 bar at 298 K.

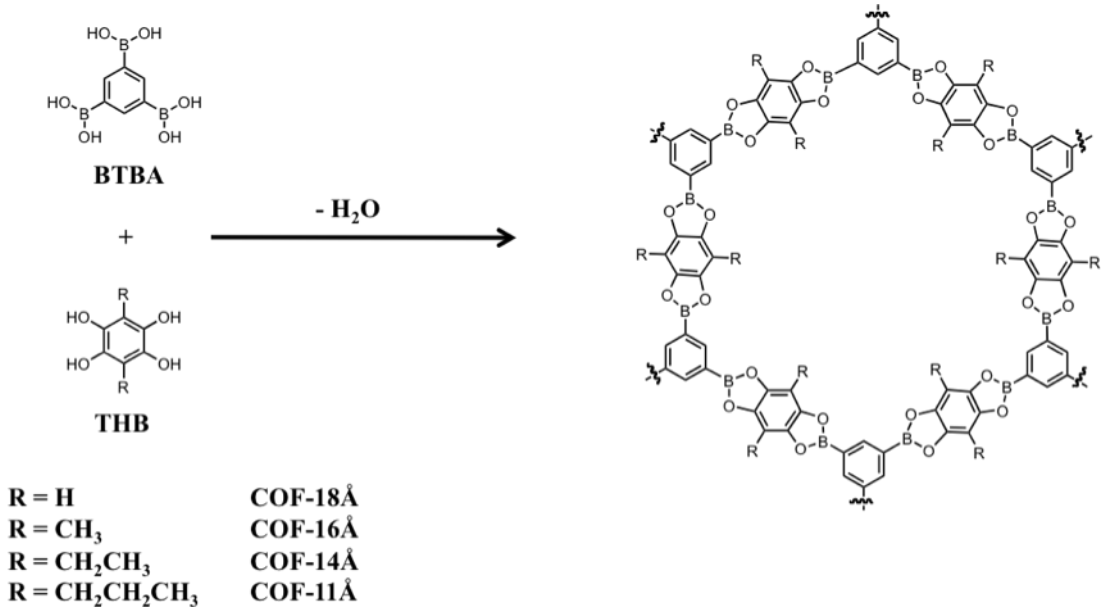

Figure 1.3. Representative alkylated functionalized COFs (Tilford, R.; Mugavero, S.; Pellechia, P.; Lavigne, J. *Adv. Mater.* **2008**, *20*, 2741-2746. Copyright Wiley-VCH Verlag GmbH & Co. KGaA. Reproduced with permission.).

1.2.2. Study of 3D boronic acid COFs as gas storage materials

The first 3D boronate ester linked COFs were prepared through the condensation of polyfunctional catechols and tetrahedral boronic acids[3,6,10] (Figure

1.4). An important feature of 3D COFs, not seen in 2D COFs, is the full accessibility of adsorption sites within the pores to all edges and faces of the polyhedra, maximizing the surface area for gas storage. The synthesis of 3D COFs by self-condensation of TBPM or TBPS to form COF-102 and COF-103, and co-condensation with HHTP to form COF-105 and COF-108, displayed volumetric densities of 0.41, 0.38, 0.18, and 0.17 g cm^{-3}, respectively[10]. Based on gas uptake studies and surface area calculations, Yaghi and colleagues concluded that 3D COFs are very porous organic materials that outperform 2D COFs in terms of their gas uptake capabilities[10].

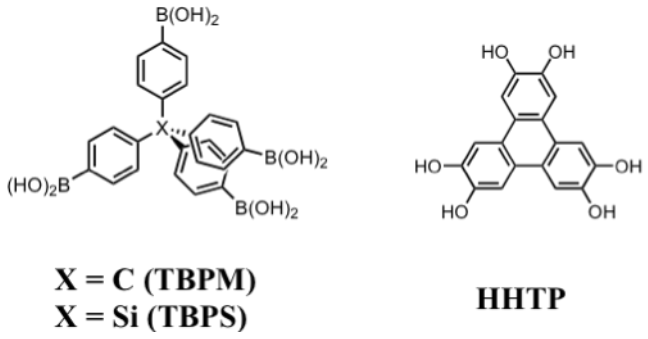

Figure 1.4. Tetrahedral boronic acid building blocks and HHTP to form 3D COFs.

In addition to synthesizing 2D COFs, Campbell and colleagues[7] synthesized COF-102 using the same microwave irradiation conditions for COF-5 to obtain a surface area of 2926 m^2 g^{-1} comparable to its reported value at 3472 m^2 g^{-1} by conventional solvothermal methods[10]. Seeking to further maximize gas absorption in 3D COFs, Lan and colleagues[11] in 2010 demonstrated that doping the pores of COF-102 and COF-103 with a lithium cation enhanced CH_4 uptake more than two times its non-doped form at 298 K. The authors attributed this phenomenon to the strong affinity of the lithium cation to CH_4 molecules by London dispersion and induced dipole interactions.

1.2.3. Miscellaneous 2D and 3D COFs as catalytic systems

In addition to boronic acid COFs, the synthesis of COFs or mesoporous networks by nitrile trimerization, transition-metal cross-coupling, imine, and borosilicate linkages has been explored. In 2008, Kuhn and colleagues[12-13] demonstrated that the use of molten $ZnCl_2$ at 400 °C leads to reversible trimerization of 1,4-dicyanobenzene (DCB) to form CTF-1 with a surface area of 791 $m^2 g^{-1}$ (Figure 1.5). Besides gas storage, CTF-1 shows promise as a catalytic device, as the high nitrogen content found in these materials yields possible coordination sites for transition metal catalysts[13].

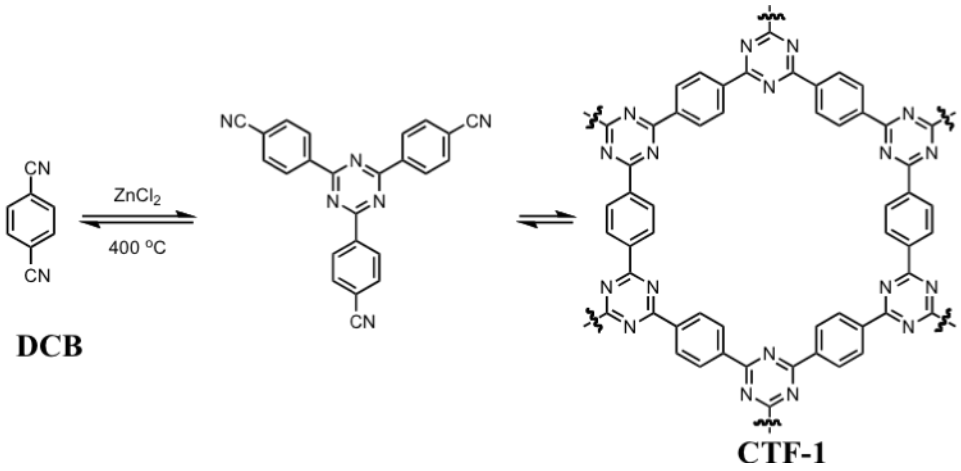

Figure 1.5. Trimerization of 1,4-dicyanobenzene in $ZnCl_2$ at 400 °C to form CTF-1 (Kuhn, P.; Antonietti, M.; Thomas, A. *Angew. Chem. Int. Ed.* **2008**, *47*, 3450-3453. Copyright Wiley VCH Verlag GmBH & Co. KGaA. Reproduced with permission.).

Another class of materials that resemble 2D COFs is amorphous mesoporous networks (CMPs) synthesized by Sonogashira-Hagihara coupling, reported by Cooper and colleagues[14] (Figure 1.6). The surface areas of these networks are significantly lower than those of reported COFs, ranging from 1018 $m^2 g^{-1}$ (CMP-0) to 512 $m^2 g^{-1}$ (CMP-5). Unlike with COFs, the synthesis of these materials is not formed by reversible conditions, which are important to crystallite growth because the sparing

solubility of building blocks controls their diffusion in solution, facilitating nucleation of a crystalline material. Thus, the presence of non-crystalline CMP networks rather than crystalline CMP networks is apparent.

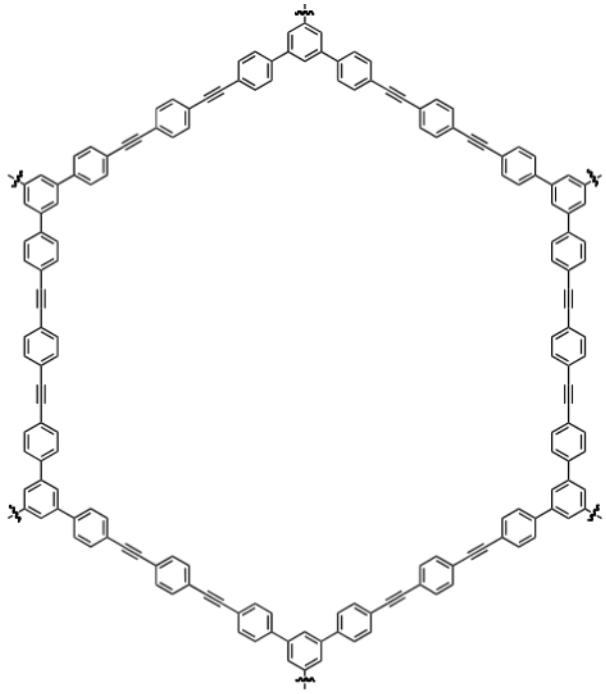

CMP-3

Figure 1.6. Representative CMP by Sonogashira-Hagihara coupling[14].

In 2008 and 2009, imine-linked (COF-300) and borosilicate-linked (COF-202) 3D COFs[15-16] were synthesized with surfaces areas of 1360 m^2 g^{-1} and 2690 m^2 g^{-1}, respectively (Figure 1.7). The silicon and nitrogen present in these COFs can act as scaffold sites for functional group attachment to create new COF materials as a result of post-synthetic modifications[16].

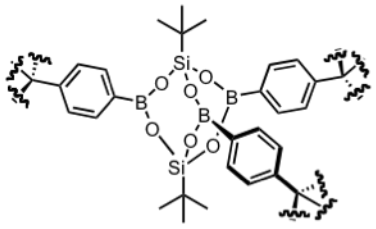

COF-202

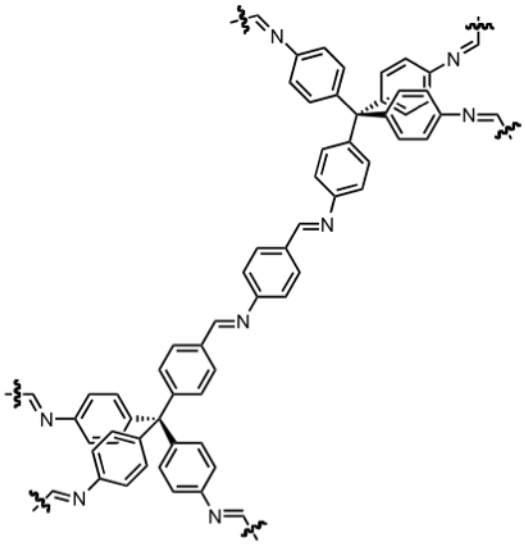

COF-300

Figure 1.7. Imine and borosilicate 3D COFs (Uribe-Romo, F.; Hunt, J.; Furukawa, H.; Klöck, C.; O'Keeffe, M.; Yaghi, O. *J. Am. Chem. Soc.* **2009**, *131*, 4570-4571; Hunt, J.; Doonan, C.; LeVangie, J.; Côté, A.; Yaghi, O. *J. Am. Chem. Soc.* **2008**, *130*, 11872-11873. Copyright American Chemical Society. Reproduced with permission.).

1.2.4. COF attachment on surfaces (SCOFs)

The first example of surface covalent organic frameworks (SCOFs) bonding onto metallic surfaces was discovered by Zwaneveld and colleagues[17], who reported that the attachment of COF-1 or COF-5 on Ag (III) led to new materials known as SCOF-1 and SCOF-2, with pore diameters of 15 Å and 29.8 Å, respectively. A disadvantage of this approach, however, is that the porosity of the networks is no longer uniform as a consequence of the annealing process, in which incomplete closure of the boroxine ring and deformation of the hexagonal polygons are observed[18]. Attempts to remove these defects were futile, illustrating that network bonding onto surfaces is a permanent process.

A yet more interesting example of COF surface chemistry is based on the surface mediated synthesis of 2D COFs using 1,3,5-tris(4-bromophenyl)benzene

(TBB) on graphite, copper, and silver surfaces described by Gulzer and colleagues[18]. The deposition of TBB on copper or silver causes homolytic dissociation of C-Br bonds, generating tri-radicals that associate to form TBB-COFs at room temperature as ordered networks on the metal surface. On the other hand, the formation of TBB-COF on graphite follows a different mechanism, in which the non-covalent self-assembly of well-ordered networks is stabilized by halogen-hydrogen bonds at elevated temperatures.

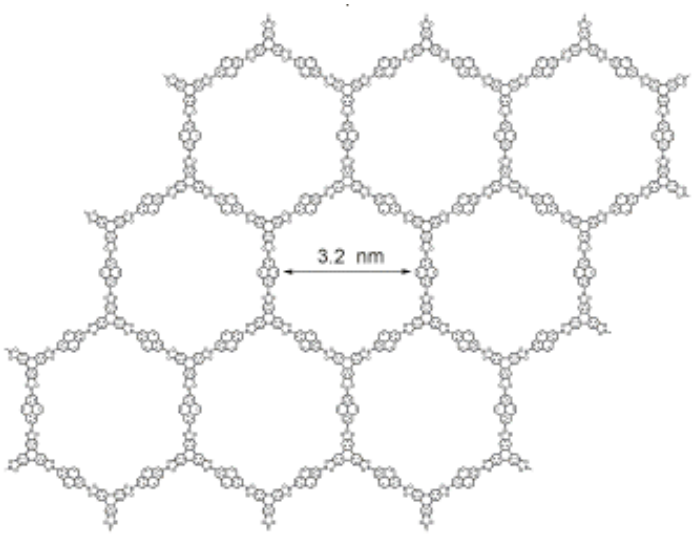

Figure 1.8. Representative photoluminescent TP-COF (Wan, S.; Guo, J.; Kim, J.; Ihee, H.; Jiang, D. *Angew. Chem. Int. Ed.* **2009**, *121*, 5547-5550. Copyright Wiley VCH Verlag GmBH & Co. KGaA. Reproduced with permission.).

1.2.5. Photoconductive COFs using π-conjugated systems

The only examples to date of photoactive COFs (TP-COF and PPy-COF) were reported by Jiang's group[1-2] in 2008 and 2009 (Figure 1.8). Due to extensive π-conjugation, these materials are highly luminescent, and capable of energy transfer. For example, according to Jiang and colleagues[1], the emission of pyrene in TP-COF and HHTP at 474 nm and 424 nm after excitation at 376 nm indicates energy transfer between pyrene and the HHTP excited state because their emissions overlap. As a

result, this is the first observation of energy transfer in a COF material. In addition, TP-COF and PPy-COF are electrically conductive, showing high photocurrent responses upon irridiation at the Au electrode[1-2].

1.3. New class of covalent organic frameworks

To date, better COFs are indeed on the horizon, and international research of COFs is already in progress. In the span of just five years, COFs have been studied for uses ranging from gas storage systems to photoactive semiconductors. Although the work on COFs as gas storage systems is noteworthy, synthesis of diverse classes of photoactive COFs is severely lacking. It is necessary to create more photoactive COFs, as organic semiconductors whose structural order is crucial for well-controlled energy and electron transfer pathways, even though their solid-state packing is difficult to predict or control. Because of their precise and predictable structures, further developing the chemistry of COFs by synthesizing *n*-type and *p*-type semiconducting building blocks is necessary.

For these reasons, the synthesis of *n*-type perylene diimides (PDI) and *p*-type oligothiophenes monomers was carried out in our laboratory. PDIs and oligothiophenes were chosen as ideal targets for incorporation into COFs because of (i) their tunable absorption in the visible spectrum, (ii) their rigid aromatic systems that can incorporate appropriate boronic acid functional groups, (iii) their formation of relatively stable radical anions or radical cations, and (iv) their excellent photostability. More important, we hypothesize that PDI and oligothiophene COFs can stack in an eclipsed arrangement similar to TP-COFs, and we anticipate electron transport pathways through these stacks.

Our strategy for designing these materials involves the introduction of boronic acid functional groups by either transition-metal borylation coupling reactions or

lithiation-borylation of the building blocks. The next two chapters, therefore, address the current methodologies used to design these new compounds.

REFERENCES

1. Wan, S.; Guo, J.; Kim, J.; Ihee, H.; Jiang, D. *Angew. Chem. Int. Ed.* **2009**, *121*, 5547-5550.

2. Wan, S.; Guo, J.; Kim, J.; Ihee, H.; Jiang, D. *Angew. Chem. Int. Ed.* **2008**, *47*, 8826-8830.

3. Mastalerz, M. *Angew. Chem. Int. Ed.* **2008**, *47*, 445-447.

4. Côté, A.; El-Kaderi, M.; Furukawa, H.; Hunt, J.; Yaghi, O. *J. Am. Chem. Soc.* **2007**, *129*, 12914-12915.

5. Han, S.; Furukawa, H.; Yaghi, O.; Goddard, W. *J. Am. Chem. Soc.* **2008**, *130*, 11580-11581.

6. Furukawa, H.; Yaghi, O. *J. Am. Chem. Soc.* **2009**, *131*, 8875-8883.

7. Campbell, N.; Clowes, R.; Ritchie, L.; Cooper, A. *Chem. Mater*. **2009**, *21*, 204-206.

8. Tilford, R.; Gemmill, W.; Loye, H.; Lavigne, J. *Chem. Mater.* **2006**, *18*, 5296-5301.

9. Tilford, R.; Mugavero, S.; Pellechia, P.; Lavigne, J. *Adv. Mater.* **2008**, *20*, 2741-2746.

10. El-Kaderi, H.; Hunt, J.; Mendoza-Cortés, J.; Côté, A.; Taylor, R.; O'Keeffe, M., Yaghi, O. *Science*. **2007**, *316*, 268-272.

11. Lan, J.; Cao, D.; Wang, W. *Langmuir*. **2010**, *26*, 220-226.

12. Kuhn, P.; Antonietti, M.; Thomas, A. *Angew. Chem. Int. Ed.* **2008**, *47*, 3450-3453.

13. Kuhn, P.; Forget, A.; Su, D.; Thomas, A.; Antonietti, M. *J. Am. Chem. Soc.* **2008**, *130*, 13333-13337.

14. Jiang, J.; Su, F.; Trewin, A.; Wood, C.; Niu, H.; Jones, J.; Khimyak, Y.; Cooper, A. *J. Am. Chem. Soc.* **2008**, *130*, 7710-7720.

15. Uribe-Romo, F.; Hunt, J.; Furukawa, H.; Klöck, C.; O'Keeffe, M.; Yaghi, O. *J. Am. Chem. Soc.* **2009**, *131*, 4570-4571.

16. Hunt, J.; Doonan, C.; LeVangie, J.; Côté, A.; Yaghi, O. *J. Am. Chem. Soc.* **2008**, *130*, 11872-11873.

17. Zwaneveld, N.; Pawlak, R.; Abel, M.; Catalin, D.; Gigmes, D.; Bertin, D.; Porte, L. *J. Am. Chem. Soc.* **2008**, *130*, 6678-6679.

18. Gutzler, R.; Walch, H.; Eder, G.; Kloft, S.; Heckl, W.; Lackinger, M. *Chem. Commun.* **2009**, *29*, 4456-4458.

CHAPTER 2:

Perylene Diimides For *n*-Type Semiconducting COFs

2.1. Abstract

The synthesis of **PDI 1** and **PDI 2** building blocks by iridium catalysis, palladium catalysis, lithium halogen exchange (LHE), and imidization in order to form **COF-PDI 1** and **COF-PDI 2** is surveyed. LHE to afford **PDI 1** boronic acids displays inconclusive results, and imidization to afford **8** as **PDI 2** is successful. Finally, the condensation between **8** and phenyl boronic acid to **10a** as a linear boronate ester provides a soluble model compound for the proposed **COF-PDI 2**.

2.2. Introduction

Perylene diimides (PDIs) and their derivatives are well-known organic dyes, used in paints and coatings[1-2]; however, their broad range of optical and electrochemical properties has also made them attractive candidates as light-harvesting materials in photovoltaic devices[3-7]. In particular, PDIs are *n*-type semiconducting materials that feature high photo and thermal stability[1,8], excellent fluorescence quantum yields[2,8], low reduction potentials[8-9], and high electron affinity, which allows them to form stable radical anions[9-10].

More importantly, appropriately functionalized PDI derivatives can form a wide variety of larger assemblies such as metallosupramolecular squares[2] or hollow cylinders[11] by π-π stacking or hydrogen bonding in solution. As described in the previous chapter, it is hypothesized that by using the strategies to form covalent organic frameworks (COFs), two-dimensional **COF-PDI 1** and **COF-PDI 2** porous materials with hexagonal networks can form via π-π stacking of the perylene units. This can be achieved using the Lewis acid catalyzed condensation of boronic acids

and acetonide-protected HHTP diols recently developed by the Dichtel group or the condensation of aryl boronic acids with 1,3-diols developed by Yaghi and colleagues[2] (Figure 2.1).

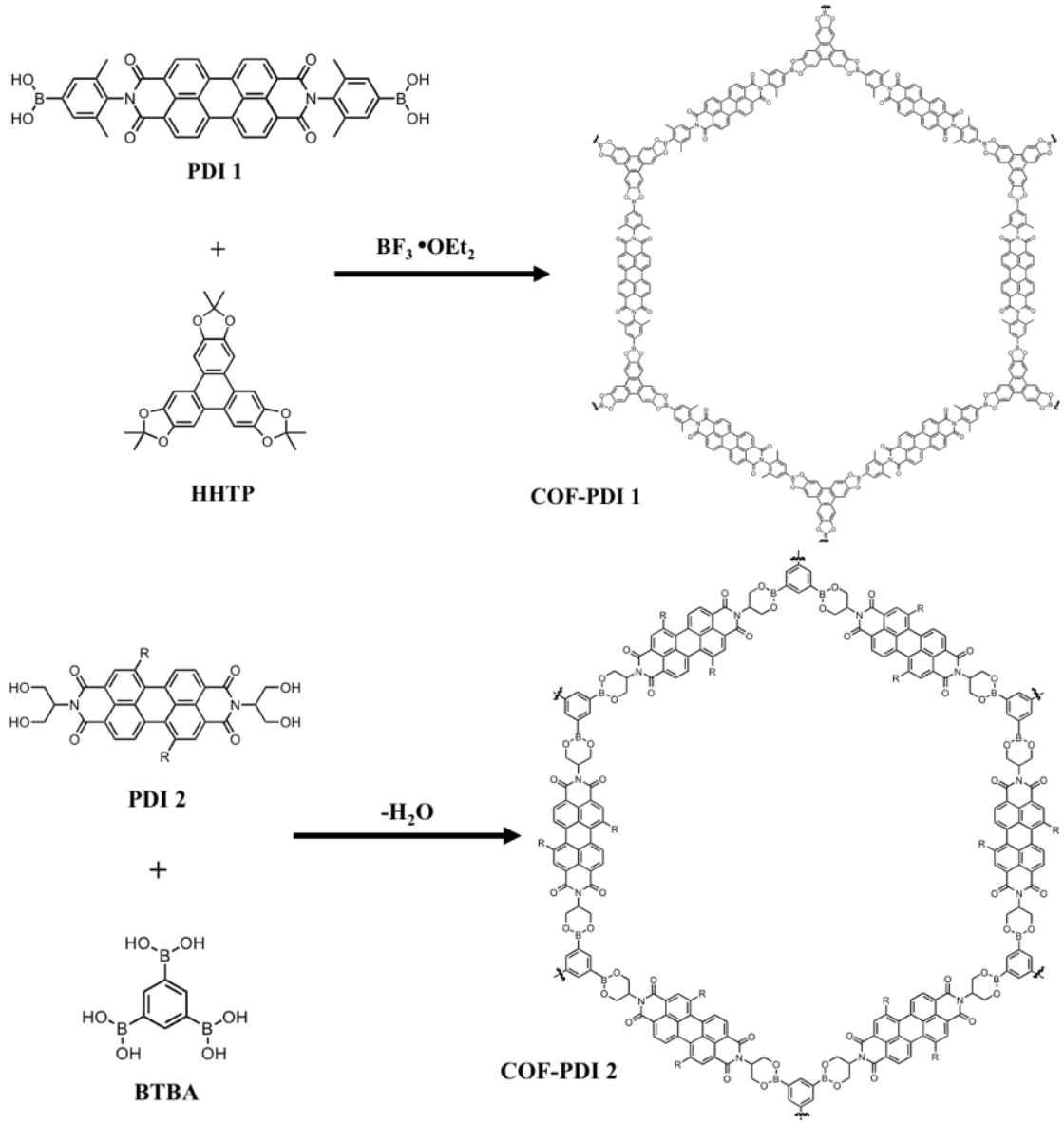

Figure 2.1. Proposed *n*-type PDI semiconducting COFs formed by π-π stacking.

In this chapter, the synthesis of *n*-type building blocks, **PDI 1** and **PDI 2**, of the proposed PDI COFs is described.

2.3. Synthetic methodologies toward PDI 1 for COF-PDI 1

To achieve the synthesis of PDI boronic acids and boronic esters, perylene dianhydrides (**PDA**) must first be converted to its imide species to allow sufficient solubility and to overcome π-π aggregation between **PDA** molecules. Using bulky aliphatic aromatic substituents, compounds **1-3** were obtained as dark red solids after recrystallization from toluene-methanol in 53-79% yields that are completely soluble in DCM and $CHCl_3$ (Figure 2.2).

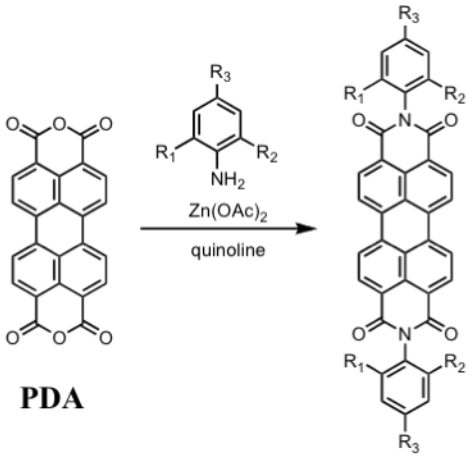

R_1, R_2 = Me R_3 = H **1**
R_1, R_3 = H; R_2 = *t*-Bu **2**
R_1, R_2 = Me; R_3 = Br **3**

Figure 2.2. Imidization of **1-3** using $Zn(OAc)_2$ in quinoline by reflux under N_2.

The success of imidization for **1**, **2**, and **3** is reflected by ^1H NMR, illustrating the characteristic doublet of doublet signals of the symmetric perylene core at 8.79, 8.78, and 8.79 ppm, respectively. In addition, new resonances in the aliphatic regions are seen at 2.18 (CH_3), 1.31 (*t*-butyl), and 2.13 (CH_3) ppm for **1**, **2**, and **3,** respectively.

A further confirmation of a PDI species is seen by MALDI-TOF MS in which analytically pure **3** has a *m/z* at 757.96 with isotope fragmentation patterns characteristic of bromine in the molecule[14]. Furthermore, FT-IR of **PDA** and **3** were taken in which C=O stretches of both species were compared (Figure 2.3).

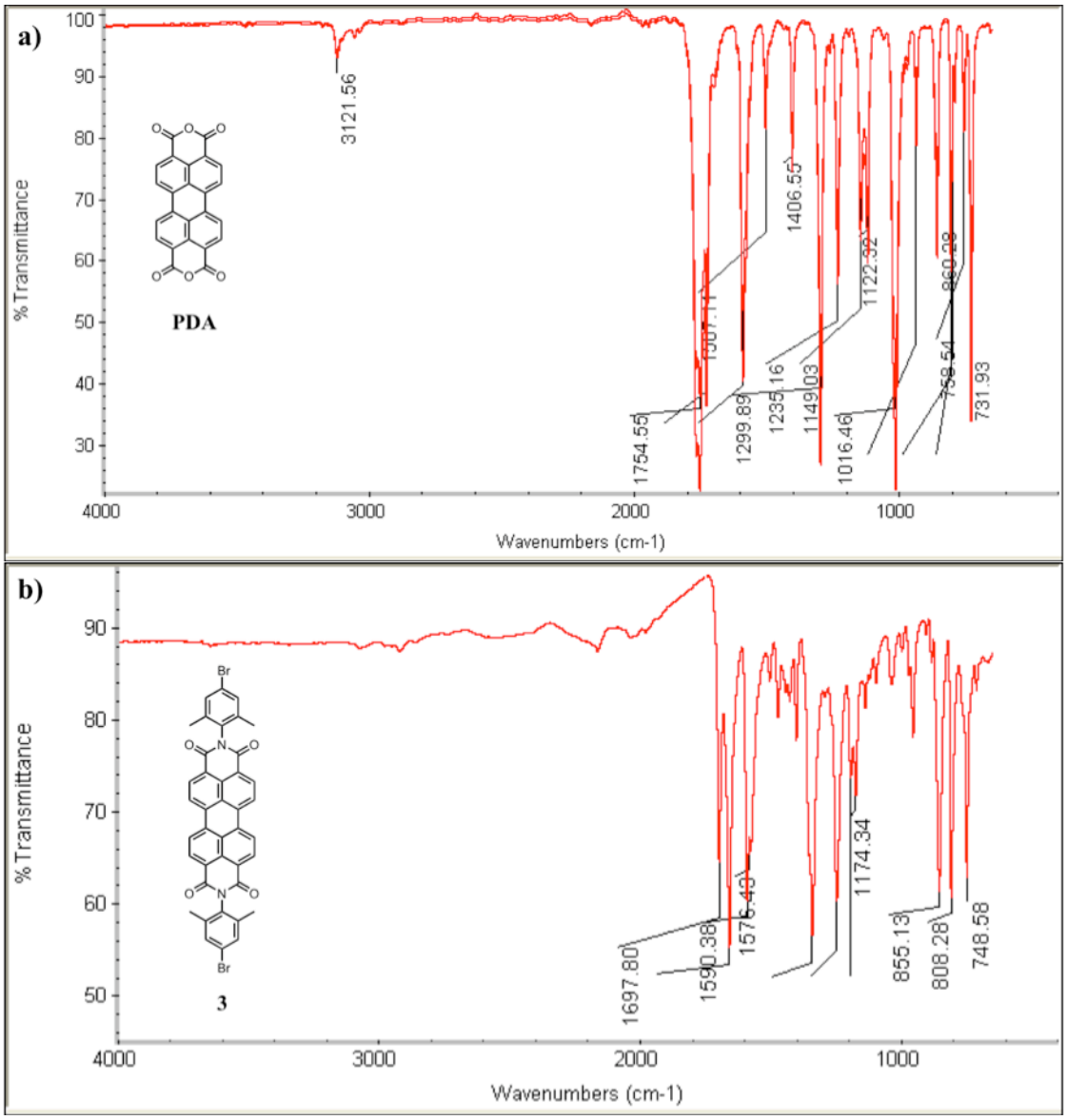

Figure 2.3. (a) FT-IR spectra of **PDA**; (b) FT-IR spectra of **3** with change in C=O stretches.

The FT-IR of **PDA** exhibits a C=O stretch of the anhydride at 1755 cm^{-1} (Figure 2.3a). However, upon imidization to **3** a new set of C=O stretches appear at 1698 and 1590 cm^{-1}, respectively (Figure 2.3b), which is the general region of imide carbonyl stretches[13-14]. Thus, FT-IR analysis indicates that imidization was successful.

Another class of PDIs was synthesized using 1,7-dibromoperylene dianhydride (**PDA-Br**) to afford **4** and **5** using a different imidization approach by refluxing the aniline species in propinoic acid overnight and recrystallizing from toluene-methanol to afford bright orange solids in 6-8% yields (Figure 2.4).

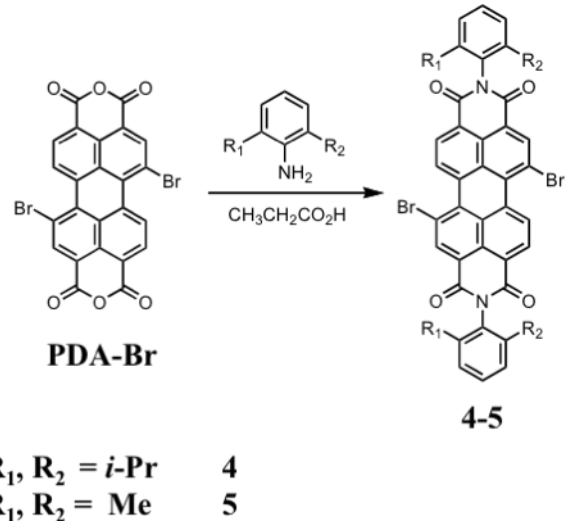

Figure 2.4. Imidization of **4** and **5** using aniline derivatives in refluxing propinoic acid.

Imidizations to **4** and **5** were successful, as evidenced by the appearance of two doublets and a singlet at 9.57, 8.81, and 9.01 ppm, respectively, in the ^1H NMR spectrum. The presence of the singlet at 9.01 ppm arises from protons at C-6 and C-12 of the perylene core caused by the attachment of bromine at C-1 and C-7. Furthermore, new resonances in the aliphatic protons for both **4** and **5** are also apparent at 2.72 (CH), 1.18 (CH_3), and 2.18 (CH_3) ppm, respectively. Finally, the

molecular weight of **4** was confirmed by MALDI-TOF MS, showing a *m/z* at 869.95 with isotope fragmentation patterns consistent for bromine groups.

In summary, the syntheses of **1**, **2**, **3**, **4**, and, **5** were successful, and these compounds were used as potential precursors to **PDI 1**.

2.3.1. Iridium catalyzed borylation to PDI 1 by C-H activation

The iridium catalyzed borylation of C-H bonds reported by Hartwig, specifically, Ir[(COD)$(OMe)_2$], is a unique catalyst because it allows the attachment of pinacol boryl groups to the least sterically hindered C-H bond with good selectivity[15-16]. Furthermore, Coventry and colleagues seem to attribute boryl selectivity to the very crowded nature of the five-coordinate *fac*-tris(boryl) species, [(Ir(bpy)$(Bpin)_3$], which is proposed as the key intermediate performing the rate-determining C-H activation step[15]. Using this approach, **1**, **2**, **4**, and **5** are likely candidates for this type of borylation at the *para* position of the aromatic ring relative to the perylene core to form **6** (Figure 2.5a). To test the reliability of iridium catalysis, we were able to reproduce the results for the borylation of pyrene (**Py**) in our lab using Coventry's method[15], in which pyrene-2,7-diboronic ester (**PyB)** was obtained as a light tan solid displaying blue luminescence under UV after purification by column chromatography (1:1 DCM: hexane) (Figure 2.5b). The same approach was used for **1**, **2**, **4**, and **5**. However, for all reaction attempts, dark red solids were obtained and identified as starting materials by ^{1}H NMR spectroscopy since there was no indication of a sharp singlet peak at 1.21 ppm representing pinacol methyl groups. Therefore, it was concluded that borylation to **6** by iridium catalysis is not the best method by which to form **PDI 1** boronic acids.

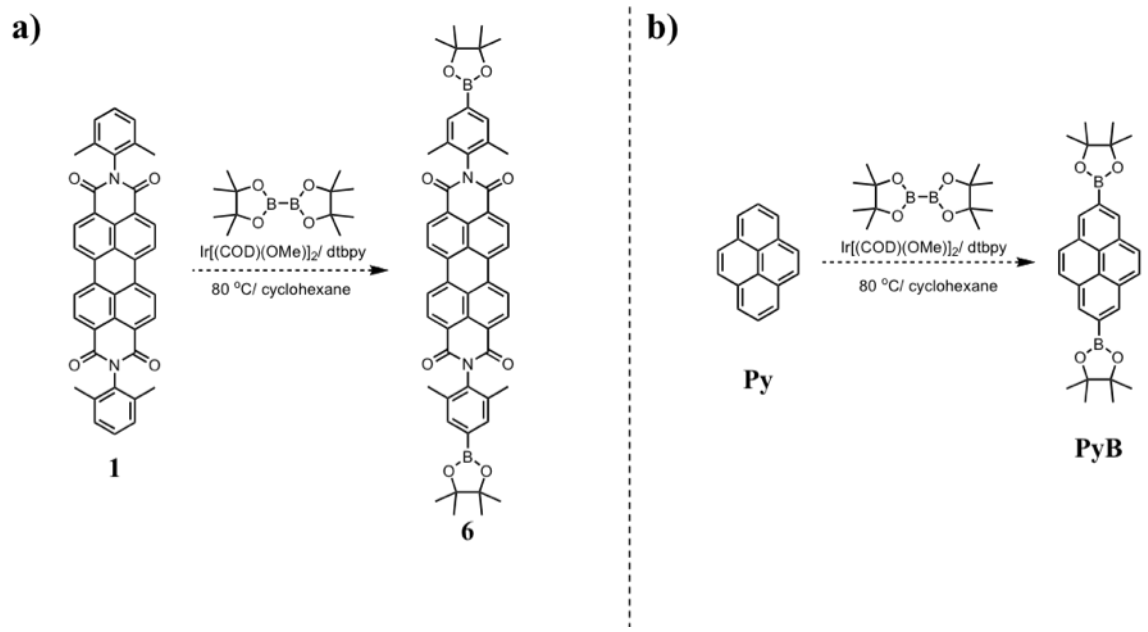

Figure 2.5. (a) Representative borylation of **1** by iridium catalyst; (b) Borylation of **Py** to **PyB** using Coventry's method.

2.3.2. Palladium catalyzed borylation to PDI 1 by aryl halide coupling

Borylation by palladium catalyst is a widely used technique first pioneered by Miyaura and colleagues[17] for cross-coupling between aryl boronic acids and aryl halides or tosylates to form biphenyl derivatives. The methodology toward borylation by palladium catalyst is often seen as a better alternative to form aryl boronic acids because of its economical tolerance to various functional groups and its insensitivity to moisture, and temperature[17-18]. Using the approach established by Broutin and colleagues[18], we performed several reaction attempts toward **6** as a **PDI 1** boronic ester using **3** as starting material (Figure 2.6).

After refluxing the solid for 16 hr, the reaction mixture was extracted following Broutin's method[18], except the crude solid was purified by column chromatography (4:1 DCM: hexane) to isolate two bright pink solids with R_f values at 0.3 and 0.07, respectively. One of the major challenges of obtaining the product is due

to the high affinity of boronic ester groups to silica gel. To remove excess bis(pinacolto)diboron (B_2Pin_2), sublimation or extraction with aqueous ammonium chloride was employed. However, despite these attempts, B_2Pin_2 was still visible by TLC as a deep purple non-fluorescent spot. In addition, characterization by multinuclear NMR spectroscopy revealed that **6** was not made but that instead a mixture of both **3** and B_2Pin_2 was evident with a sharp singlet at 1.24 ppm (^{1}H NMR) and 36.3 ppm (^{11}B NMR), respectively. This seems to indicate that borylation by a palladium catalyst with **3** did not work.

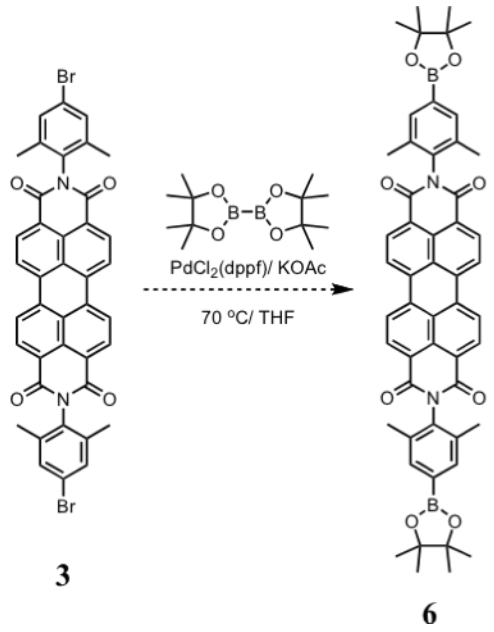

Figure 2.6. Attempted palladium catalyzed borylation of **3** to afford **PDI 1** boronic ester.

To increase the effectiveness of borylation by palladium catalyst, one should synthesize **3** using aniline derivatives with better leaving groups such as 4-iodoaniline or 4-tosylaniline to drive the reaction more vigorously to completion. This was attempted in our lab as preliminary work, and further investigation should be undertaken to determine its reliability.

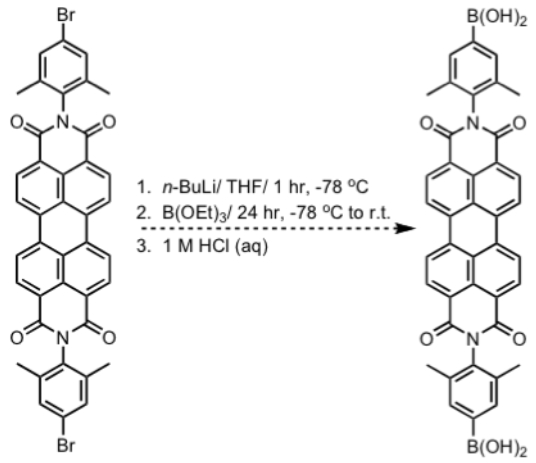

Figure 2.7. Lithium halogen exchange of **3** using triethylborate in THF.

2.3.3. Borylation by lithium halogen exchange (LHE)

Lithium halogen exchange (LHE) is one of the most powerful borylation reactions available, but its high reactivity, low tolerance to functional groups (CO_2H, COH, COR, $CONH_2$, RNH_2), and sensitivity to moisture and air render this technique challenging. LHE reaction conditions and an acidic workup[19] were employed using **3**, and the resulting crude product was triturated with hexane to afford a black-red solid that is believed to be **7** (Figure 2.7). Characterization of this compound by ^{1}H NMR spectroscopy was difficult to obtain, leading to complex and often ambiguous signals in the aromatic region. In addition, its ^{11}B NMR spectrum seems to indicate the presence of unidentifiable boron species with chemical shifts at 35.6 and 23.4 ppm. It is likely that the signal seen at 23.4 ppm is not triethylborate, which has a signal at 21.0 ppm in acetone-*d6* when characterized in our laboratory. Using dithranol as a matrix, the MALDI-TOF MS result is also ambiguous, with a *m/z* at 652.0 of the crude product instead of the desired *m/z* 686.2, because it does not reflect **7** being formed nor

its boronic ester derivative, with a predicted *m/z* at 742.4. In summary, the synthesis of **PDI 1** boronic acid by LHE is inconclusive, and further investigation to study these reaction conditions should be considered.

2.4. Synthetic methodologies toward PDI 2 for COF-PDI 2

Given the failure of several approaches to provide boronic acid functionalized PDI derivatives, an alternative strategy was initiated by synthesizing PDI 1,3-diols as **PDI 2**, which can be used as a precursor to form **COF-PDI 2** after condensation with BTBA. In this work, the synthesis of **PDI 2** by imidization of **PDA** and 2-amino-1,3-propanediol in pyridine was achieved using zinc acetate as catalyst to form **8** as a dark red solid in excellent yield (Figure 2.8a). Based on FT-IR and MALDI-TOF MS, the broad OH stretch at 3467 cm^{-1} and sharp imide C=O stretches at 1686 and 1640 cm^{-1}, respectively, are clear indications that **8** was obtained with a *m/z* at 540.3 (Figure 2.8b). However, its ^{1}H NMR spectrum could not be obtained because of its insolubility in common organic solvents.

Recently, in the Dichtel group, efforts are underway to form COFs using boron trifluoride etherate (BF_3•OEt_2) as a Lewis acid catalyst to condense acetonide protected diols and aryl boronic acids to boronate esters. Using this concept, the hydroxyl groups of **8** were protected with 2,2-dimethoxypropane using PTSA as catalyst in DMF after heating at 120 ºC in a flame-sealed ampule for 24 hr to afford a dark red solid after filtration (Figure 2.9).

Based on MALDI-TOF MS, although the desired product **9b** was formed with a *m/z* of 617.2, the presence of **9a** at a *m/z* of 577.3 indicates the reaction did not go to completion, especially with the presence of **8** at a *m/z* of 537.3 (Figure 2.10). In order to allow complete conversion of **8** to **9b**, an alternative approach to the synthesis of acetonide protected PDIs would be to protect the diol groups of 2-amino-1,3-

propanediol with 2,2-dimethoxypropane first and then subject this compound to imidization with **PDA** using zinc acetate to form the desired product as **9b**.

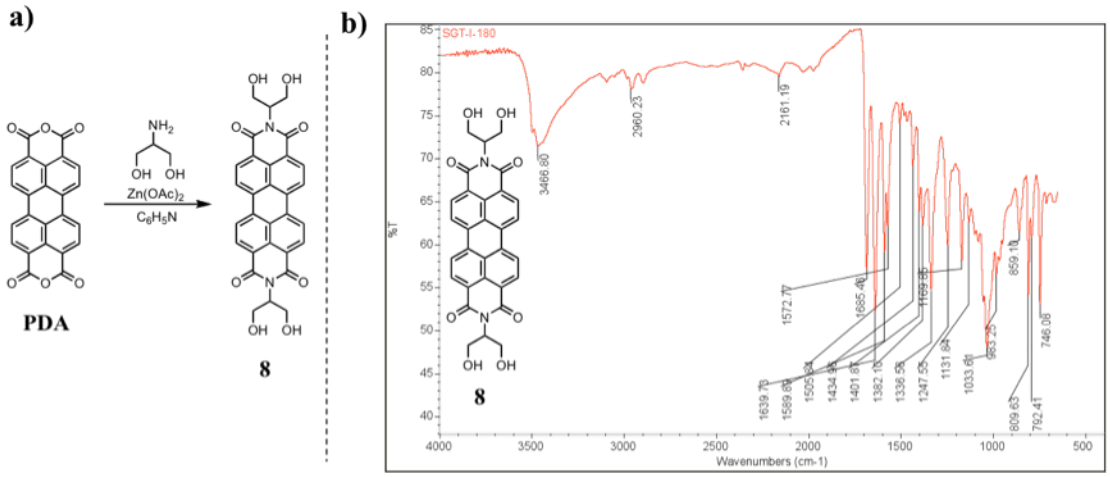

Figure 2.8. (a) Imidization of **PDA** to **8** using $Zn(OAc)_2$ as catalyst; (b) FT-IR spectra of **8**.

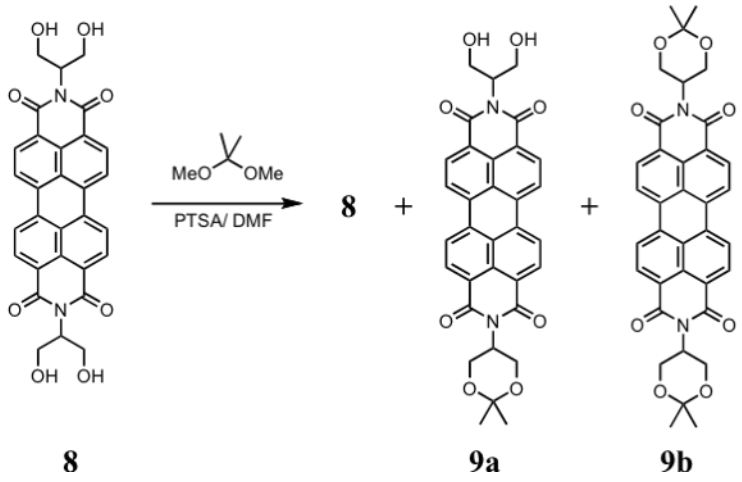

Figure 2.9. Attempted synthesis to acetonide protected **9** using 2,2-dimethoxypropane.

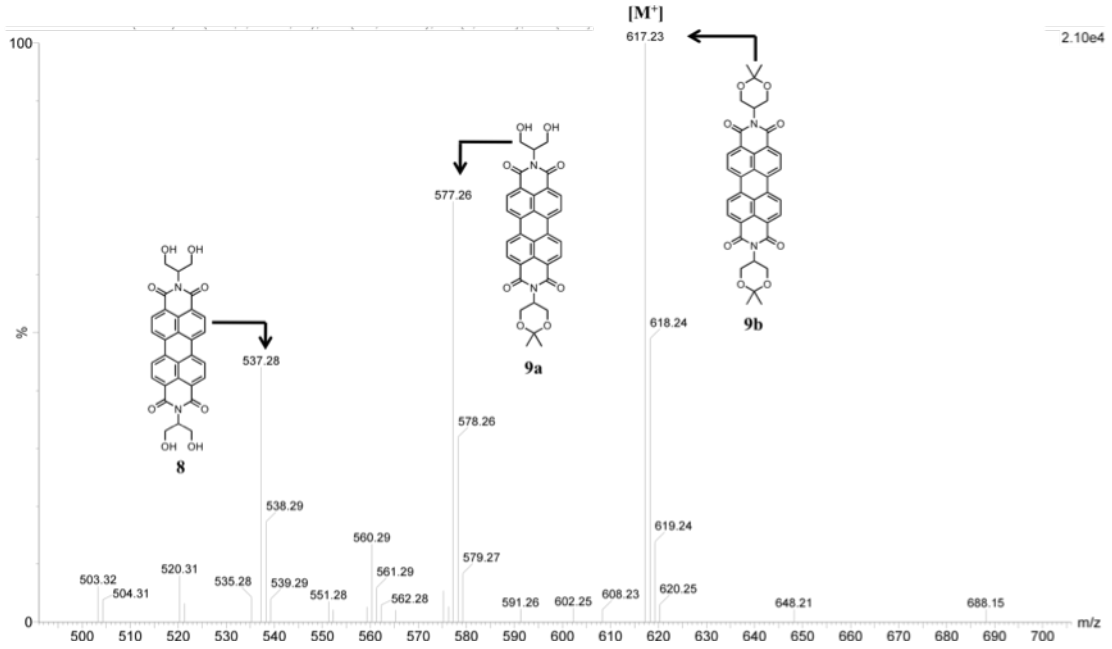

Figure 2.10. MALDI-TOF MS of compound **9** (crude).

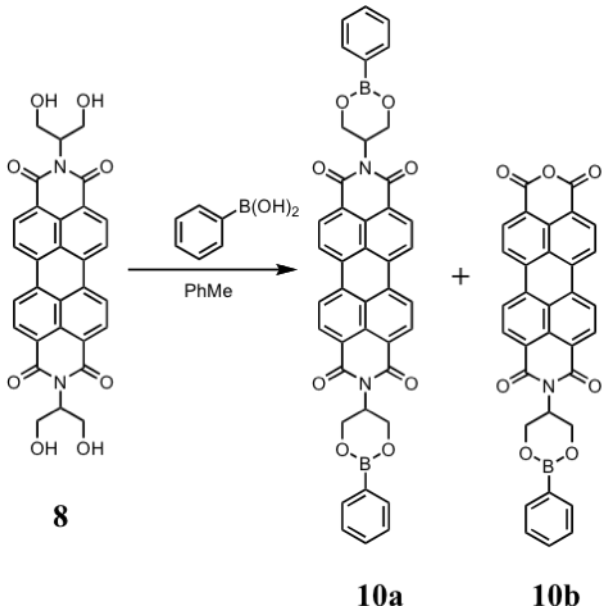

Figure 2.11. Thermal dehydration of **8** and phenylboronic acid in toluene to **10**.

Finally, to test whether **COF-PDI 2** is likely to form, **10a** was synthesized as a model compound following Rambo and colleagues'[20] procedure by condensation of

phenylboronic acid and **8** in toluene using a Dean Stark apparatus to afford a dark red solid after solvent removal *in vacuo* (Figure 2.11). The condensation reaction was somewhat successful, using three equivalents of phenylboronic acid to obtain **10a** with a *m/z* at 712.5, although **8** and its monoboronic ester form **10b** are still evident in the spectra with a *m/z* at 540.4 and 551.5, respectively (Figure 2.12). Thus, these preliminary results suggest that **10a** is a good model for the synthesis of **COF-PDI 2** using BTBA instead.

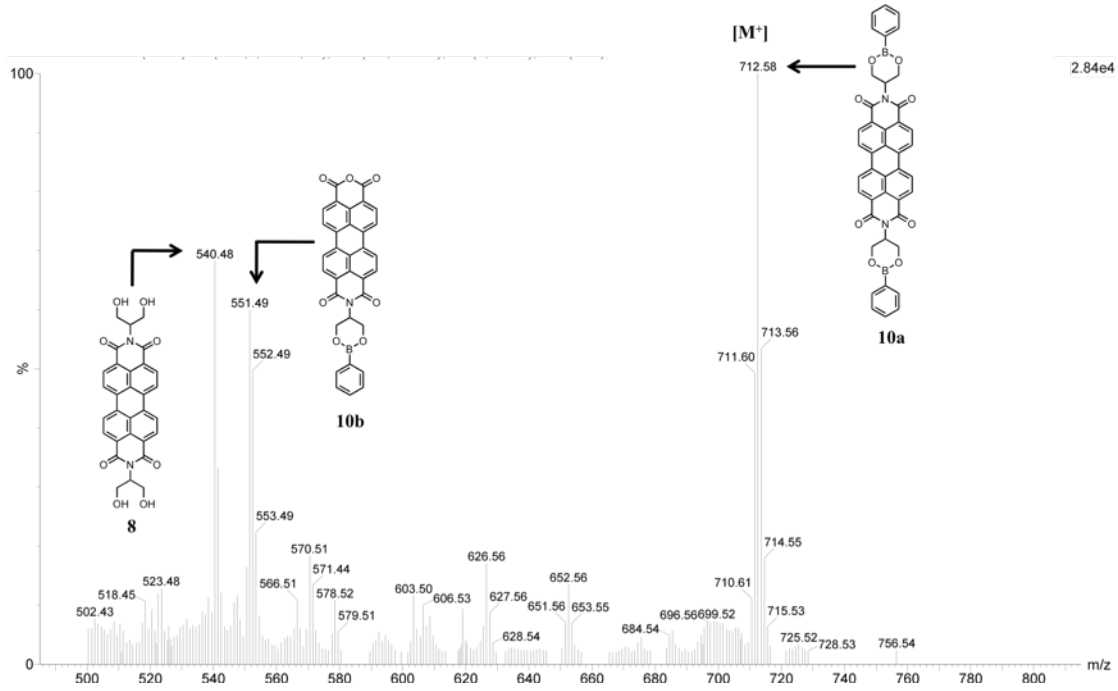

Figure 2.12. MALDI-TOF MS of compound **10** (crude).

2.5. Future work and conclusions

In order to design **COF-PDI 1**, new synthetic protocols or improvement of existing protocols to create PDI boronic acids or esters as **PDI 1** should be considered because iridium catalysis, palladium catalysis, and LHE to afford **6** or **7** did not work. On the other hand, compounds **8** and **10a** seem to be the most promising PDI monomers for **COF-PDI 2**. Thus, efforts are currently in progress to optimize the

reaction conditions for **PDI 1** and **PDI 2**, which will then be used to synthesize the proposed COFs using existing protocol [12,21] or Lewis acid catalysis.

2.6. Experimental section

2.6.1 General considerations

All manipulations were carried out under a nitrogen atmosphere using flame-dried glassware following standard vacuum line and Schlenk techniques. All compounds unless otherwise stated were purchased from Sigma Aldrich and Alfa Aesar and used as received. Methanol, tetrahydrofuran, N,N-dimethylformamide, and toluene were obtained from a custom-built alumina column solvent purification system. ^{1}H, ^{13}C, and ^{11}B NMR were obtained on a 300 MHz Bruker Avance NMR spectrometer using $CDCl_3$ as the solvent. FT-IR measurements were taken on a Nicolet iS10 FT-IR spectrometer from Thermo Fisher Scientific. MALDI-TOF measurements were taken on a Waters MALDI Micro MX spectrometer on negative-mode ionization using dithranol as the matrix.

N,N-Di(2,6-dimethylphenyl)-perylene-3,4:9,10-tetracarboxylic acid bisimide (1): Compound **1** was synthesized following a modified procedure reported by Huang et al[23]. To a 50 mL round-bottom flask equipped with a magnetic stirbar, condenser, and nitrogen inlet were added perylene-3,4:9,10-tetracarboxylic acid bisanhydride (0.834 g, 2.126 mmol), zinc acetate (0.300 g, 1.635 mmol), and 2,6-dimethylaniline (1.546 g, 12.755 mmol), dissolved in quinoline (15 mL) that was refluxed for 16 hrs. After cooling to room temperature, the reaction mixture was precipitated in 2:1 CH_3OH: 10% HCl (300 mL) that was stirred for 1 hr, forming a red solid, which was filtered and washed with CH_3OH (3 x 10 mL). The crude solid was poured into 10% Na_2CO_3 (94 mL) and allowed to stir for 1 hr at 0 °C, and was filtered and washed repeatedly with H_2O to remove excess aniline until the filtrate changed from neon green to

magenta and, finally, turned colorless. The red solid was dried under high vacuum at 100 °C overnight and further purified by recrystallization from toluene-methanol to afford **1** as a dark red solid (0.388 g, 53%). ^{1}H NMR (300 MHz, $CDCl_3$): ∂ 8.79 (dd, J = 7.97 Hz; 7.97 Hz, 8H), 7.32 (s, 4H), 7.30 (s, 2H); 2.18 (s, 12H).

N,N-Di(4-*tert*-butylphenyl)-perylene-3,4:9,10-tetracarboxylic acid bisimide (2): Compound **2** was synthesized following a modified procedure reported by Huang et al[23]. To a 250 mL round-bottom flask equipped with a magnetic stirbar, condenser, and nitrogen inlet were added perylene-3,4:9,10-tetracarboxylic acid bisanhydride (2.780 g, 7.086 mmol), zinc acetate (1.000 g, 5.451 mmol), and 4-*tert*-butylaniline (6.345 g, 42.516 mmol), dissolved in quinoline (67 mL) that was refluxed for 16 hrs. After cooling to room temperature, the reaction mixture was precipitated in 2:1 CH_3OH: 10% HCl (1400 mL) that was stirred for 1 hour, forming a purple-red solid that was filtered and washed with CH_3OH (3 x 100 mL). The crude solid was poured into 10% Na_2CO_3 (100 mL) and allowed to stir for 1 hr at 0 °C, and was filtered and washed repeatedly with H_2O to remove excess aniline until the filtrate changed from neon green to magenta and, finally, turned colorless. The red solid was dried under high vacuum at 100 °C overnight and further purified by recrystallization from toluene-methanol to afford **2** as a dark red solid (2.80 g, 79%). ^{1}H NMR (300 MHz, $CDCl_3$): ∂ 8.78 (dd, J = 7.97 Hz; 7.97 Hz, 8H), 7.67 (d, J = 7.50 Hz, 2H), 7.46 (t, J = 7.50 Hz, 2H); 7.43 (t, J = 7.32 Hz, 2H), 7.12 (d, J = 7.32 Hz, 2H), 1.31 (s, 18H).

N,N-Di(4-bromo-2,6-dimethylphenyl)-perylene-3,4:9,10-tetracarboxylic acid bisimide (3): Compound **3** was synthesized following the same procedure as compound **2** using perylene-3,4:9,10-tetracarboxylic acid bisanhydride (2.000 g, 5.098 mmol), zinc acetate (1.216 g, 6.627 mmol), and 4-bromo-2,6-dimethylaniline (7.956 g,

39.763 mmol) to afford **3** as a dark red solid (2.01 g, 52%). FT-IR (neat): 2921, 2851, 1702, 1657, 1593, 1577, 1505, 1433, 1402, 1357, 1255, 1181, 1123, 1090, 968, 850, 808, 743, 691 cm^{-1}; ^1H NMR (300 MHz, $CDCl_3$): ∂ 8.79 (dd, J = 7.68 Hz, 7.89 Hz, 8H), 7.39 (s, 4H), 2.13 (s, 12H); MALDI-TOF calcd for $[C_{40}H_{24}Br_2N_2O_4]^+$ 756.01, found 757.96.

N,N-Di(2,6-diisopropylphenyl)-1,7-dibromoperylene-3,4:9,10-tetracarboxylic acid bisimide (4): Compound **4** was synthesized following a modified procedure reported by Rohr et al[24]. 1,7-dibromoperylene-3,4:9,10-tetracarboxylic acid bisanhydride was synthesized using the method reported by Würthner et al[25]. To a 250 mL round-bottom flask equipped with magnetic stirbar, condenser, and nitrogen inlet were added 1,7-dibromoperylene-3,4:9,10-tetracarboxylic acid bisanhydride (5.000 g, 9.089 mmol) and 2,6-diisopropylaniline (7.251 g, 40.901 mmol) in propinoic acid (115 mL) that was heated at 160 °C for 16 hrs. The reaction mixture was filtered while hot through a G4 glass frit and washed with hot propinoic acid (2 x 50 mL). The red-brown filtrate was then poured into H_2O (100 mL) to afford a bright red-pink precipitate, which was filtered and purified by recrystallization from toluene-methanol to afford **4** as a bright orange solid (0.435 g, 6%). ^1H NMR (300 MHz, $CDCl_3$): ∂ 9.57 (d, J = 8.16 Hz, 2H), 9.01 (s, 2H), 8.81 (d, J = 8.16 Hz, 2H), 7.51 (t, J = 7.77 Hz, 2H), 7.36 (d, J = 7.77 Hz, 4H), 2.72 (m, 4H), 1.18 (d, J = 6.91 Hz, 24H); MALDI-TOF calcd for $[C_{48}H_{40}Br_2N_2O_4]^+$ 868.13, found 869.95.

N,N-Di(2,6-dimethylphenyl)-1,7-dibromoperylene-3,4:9,10-tetracarboxylic acid bisimide (5): Compound **5** was synthesized following the same procedure as compound **4** using 1,7-dibromoperylene-3,4:9,10-tetracarboxylic acid bisanhydride (5.000 g, 9.089 mmol) and 2,6-dimethylaniline (4.956 g, 40.901 mmol) in propinoic

acid (115 mL) to afford **5** as a red-orange solid (0.527 g, 8%). ^{1}H NMR (300 MHz, $CDCl_3$): ∂ 9.56 (d, J = 7.43 Hz, 2H), 8.99 (s, 2H), 8.79 (d, J = 7.43 Hz, 2H), 7.22 (s, 6H), 2.18 (s, 12H).

N,N-Di(1,3-propanediol)-perylene-3,4:9,10-tetracarboxylic acid bisimide (8): To a 50 mL round-bottom flask equipped with magnetic stirbar and nitrogen inlet were added perylene-3,4:9,10-tetracarboxylic acid bisanhydride (0.200 g, 0.510 mmol), 2-amino-1,3-propanediol (0.362 g, 3.976 mmol), and zinc acetate (0.122 g, 0.663 mmol) in pyridine (20 mL) that was allowed to reflux overnight. The reaction mixture was poured into H_2O (75 mL) to precipitate a maroon-red solid that was stirred for 15 min, filtered, and washed with CH_3OH (2 x 20 mL). The solid was dried under high vacuum at 100 °C to afford **11** as a maroon-red solid (0.323 g, 80%). FT-IR (neat): 3467, 2960, 2161, 1665, 1640, 1590, 1573, 1506, 1435, 1402, 1382, 1337, 1248, 1170, 1132, 1034, 963, 859, 810, 792, 746 cm^{-1}; MALDI-TOF calcd for $[C_{30}H_{22}N_2O_8]^+$ 538.14, found 540.30.

APPENDIX

The following section includes MALDI and ^{1}H NMR spectra for characterization of compounds **1**, **2**, **3**, **4**, **5**, and **8**. All spectra were recorded based on considerations mentioned in section 2.6.

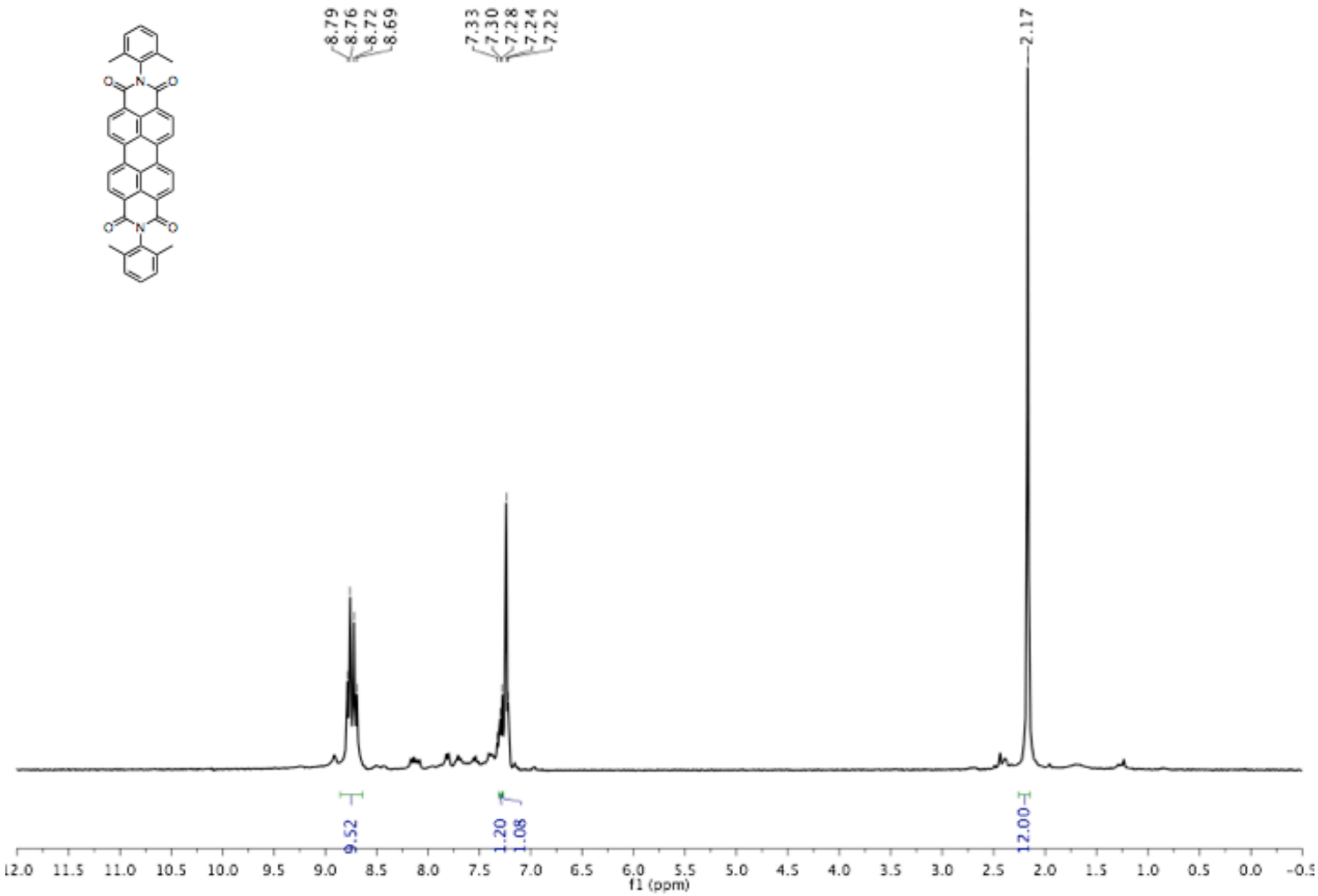

Appendix Figure 2.1. ^{1}H NMR of compound **1** in $CDCl_3$

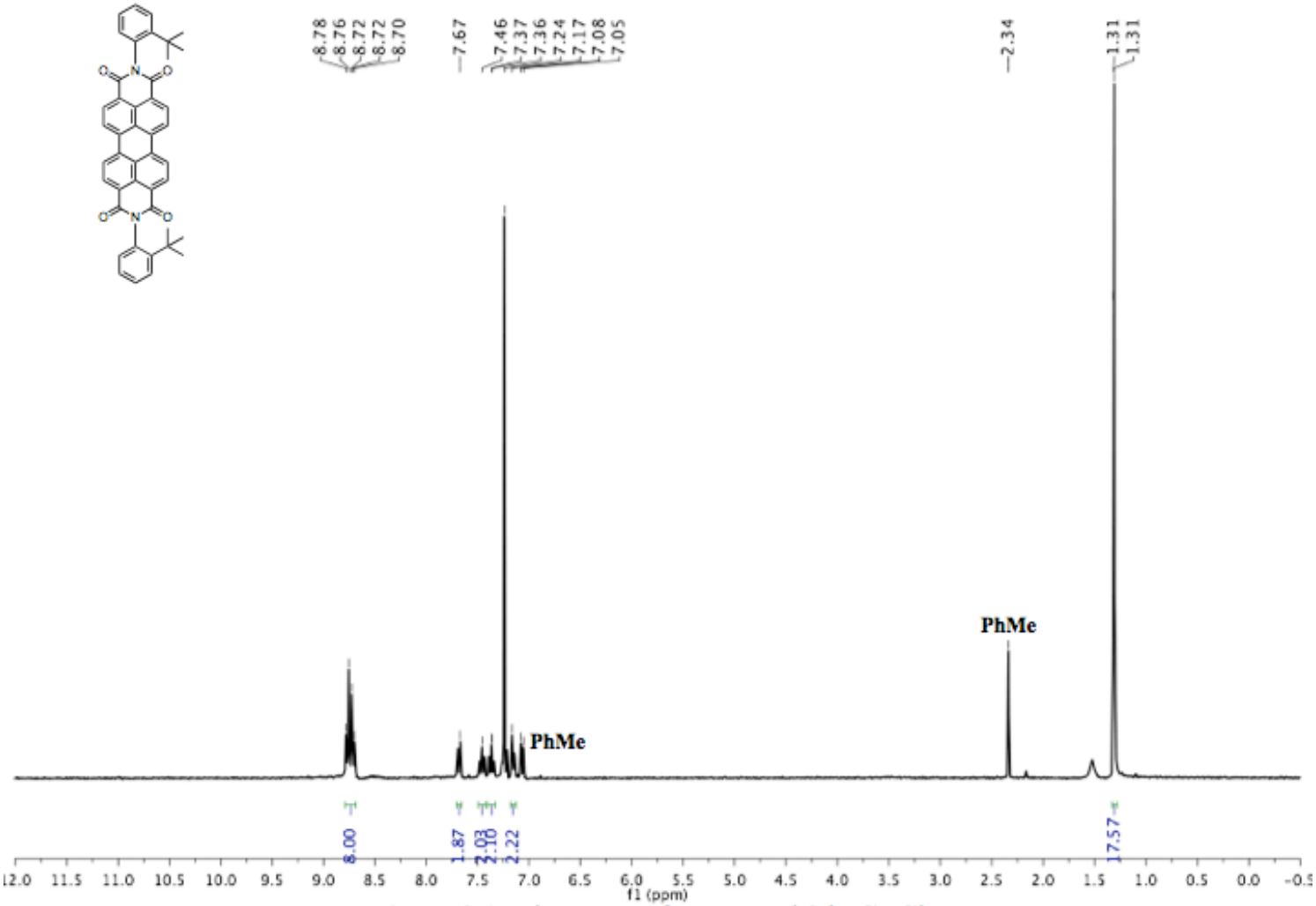

Appendix Figure 2.2. ^{1}H NMR of compound **2** in $CDCl_3$

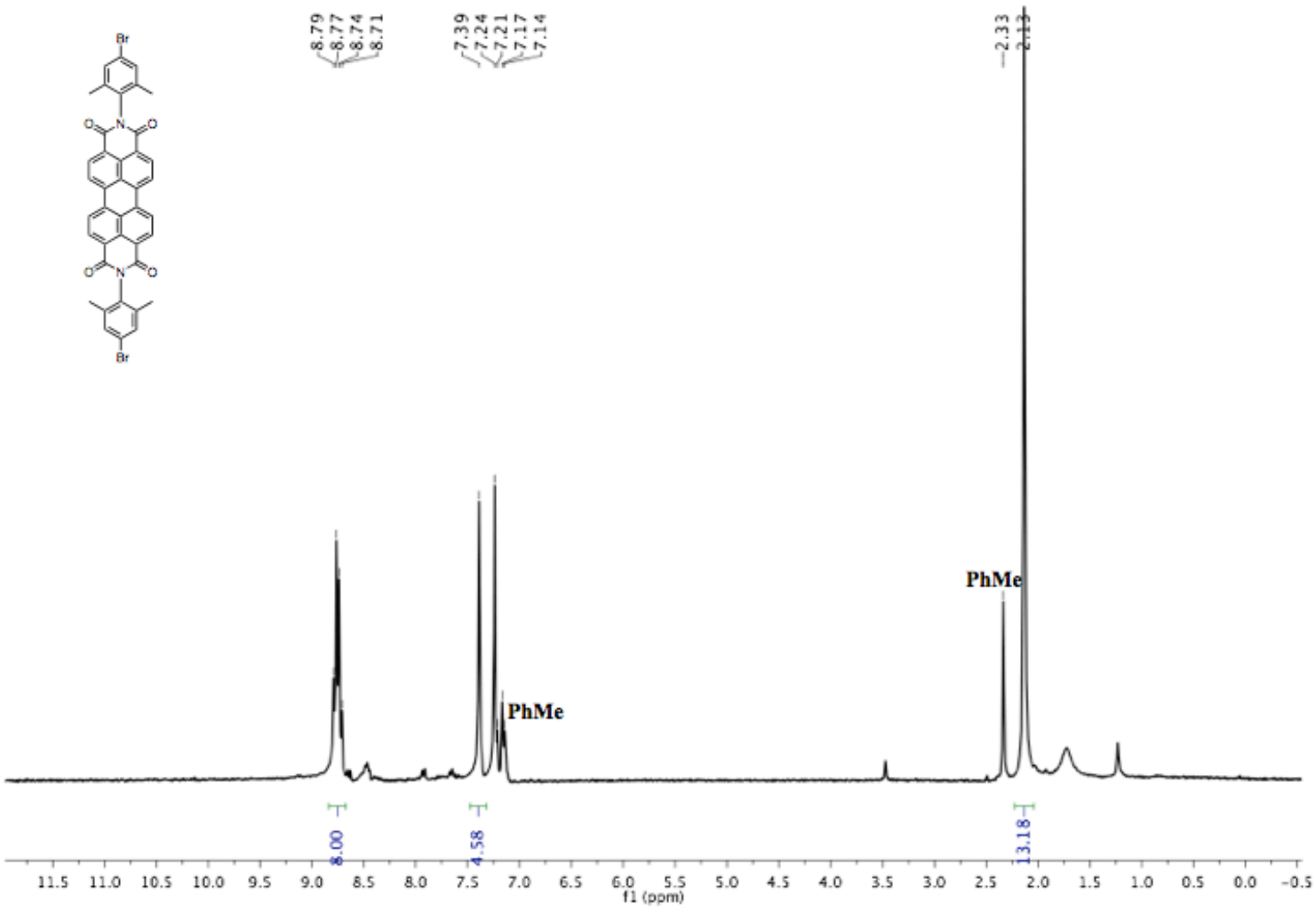

Appendix Figure 2.3. ^{1}H NMR of compound **3** in $CDCl_3$

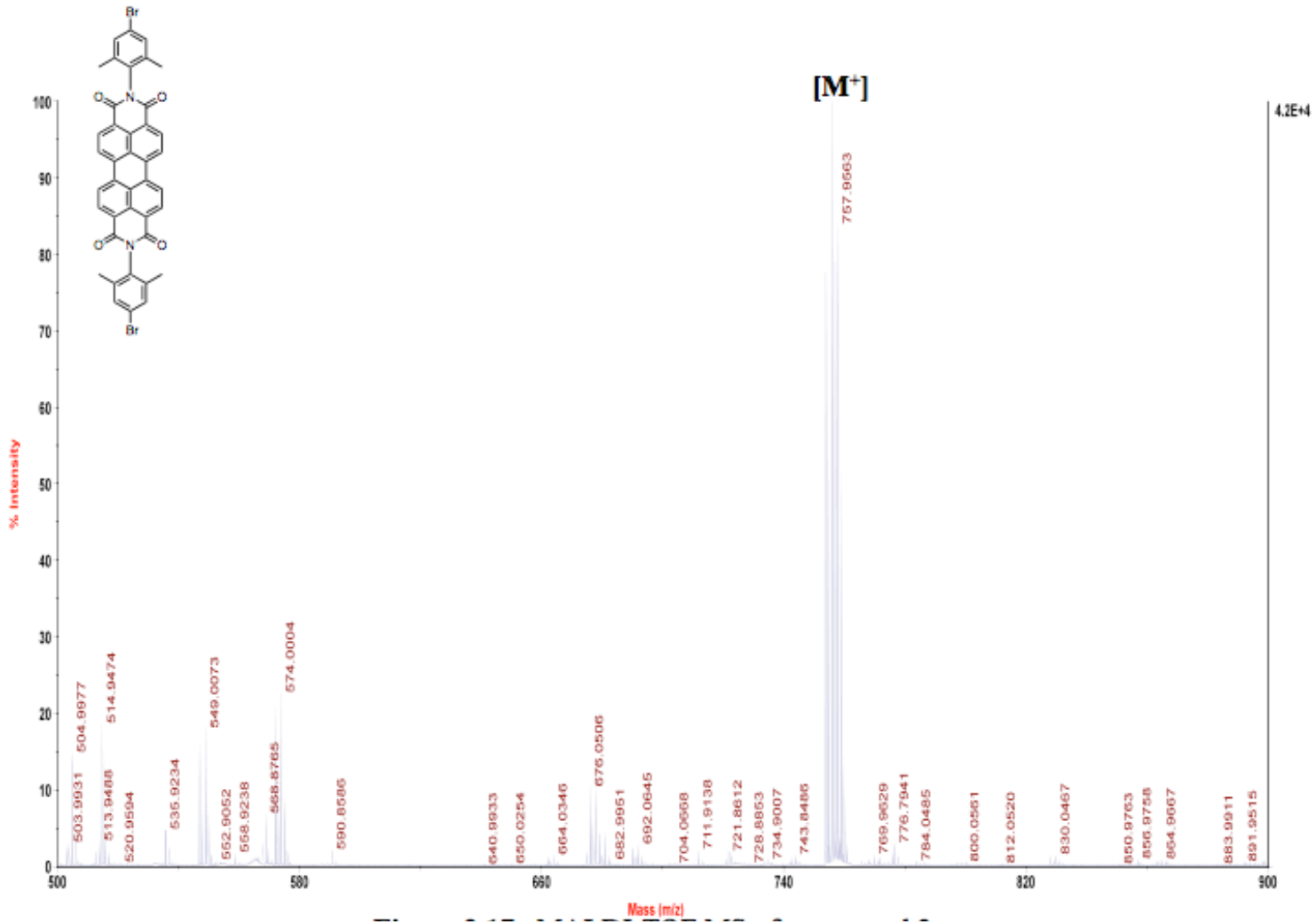

Appendix Figure 2.4. MALDI-TOF MS of compound **3**

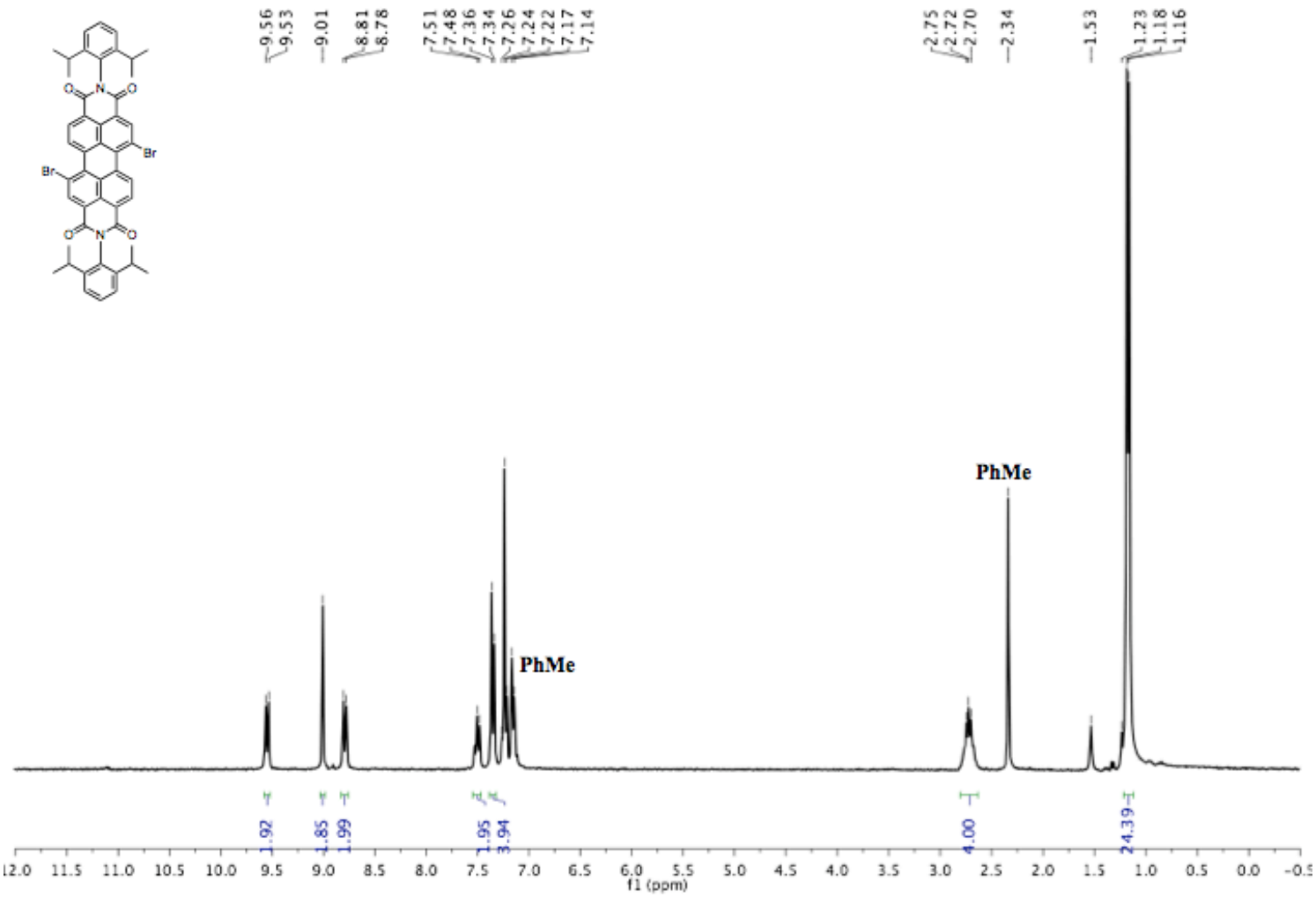

Appendix Figure 2.5. ^{1}H NMR of compound **4** in $CDCl_3$

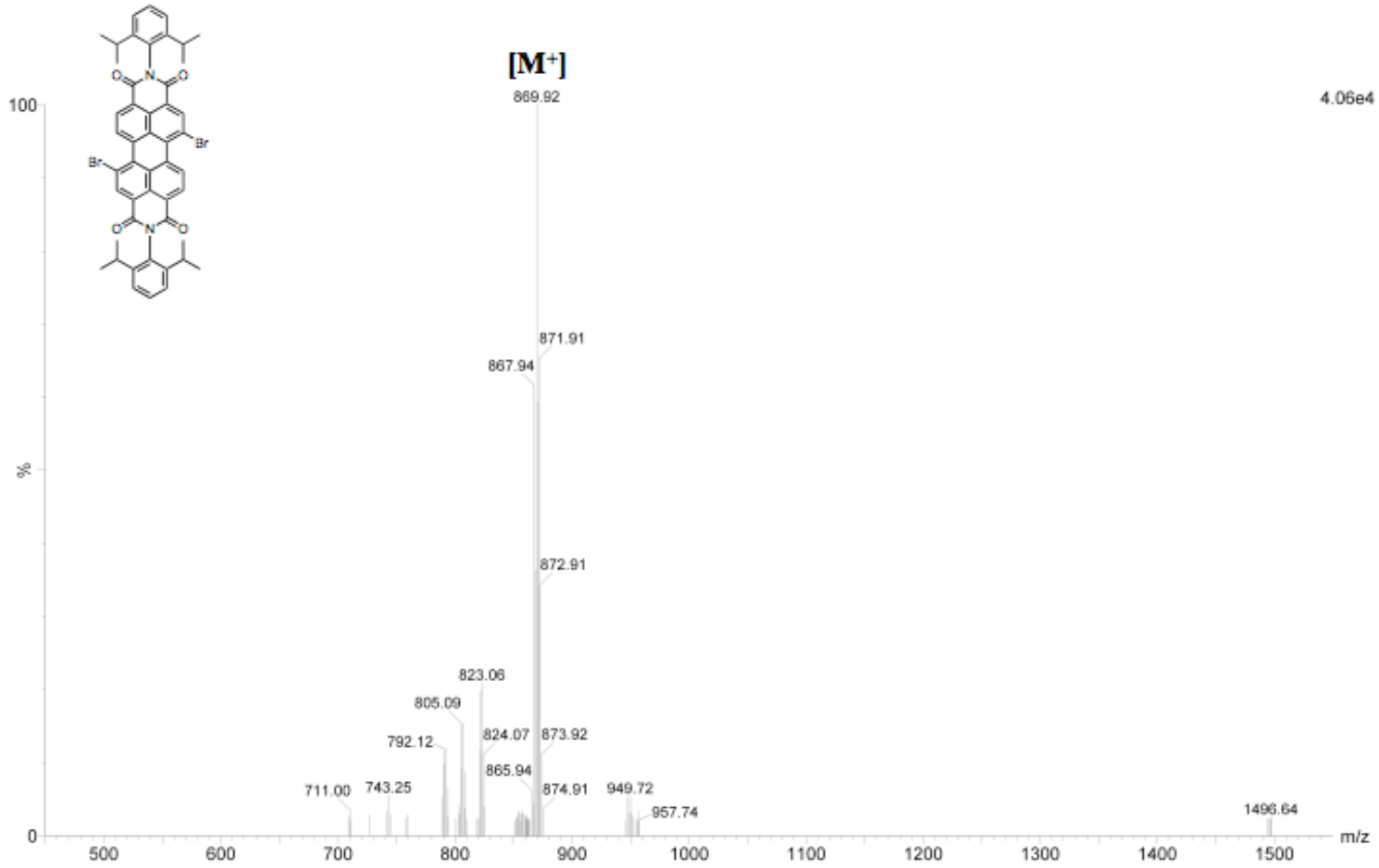

Appendix Figure 2.6. MALDI-TOF MS of compound **4**

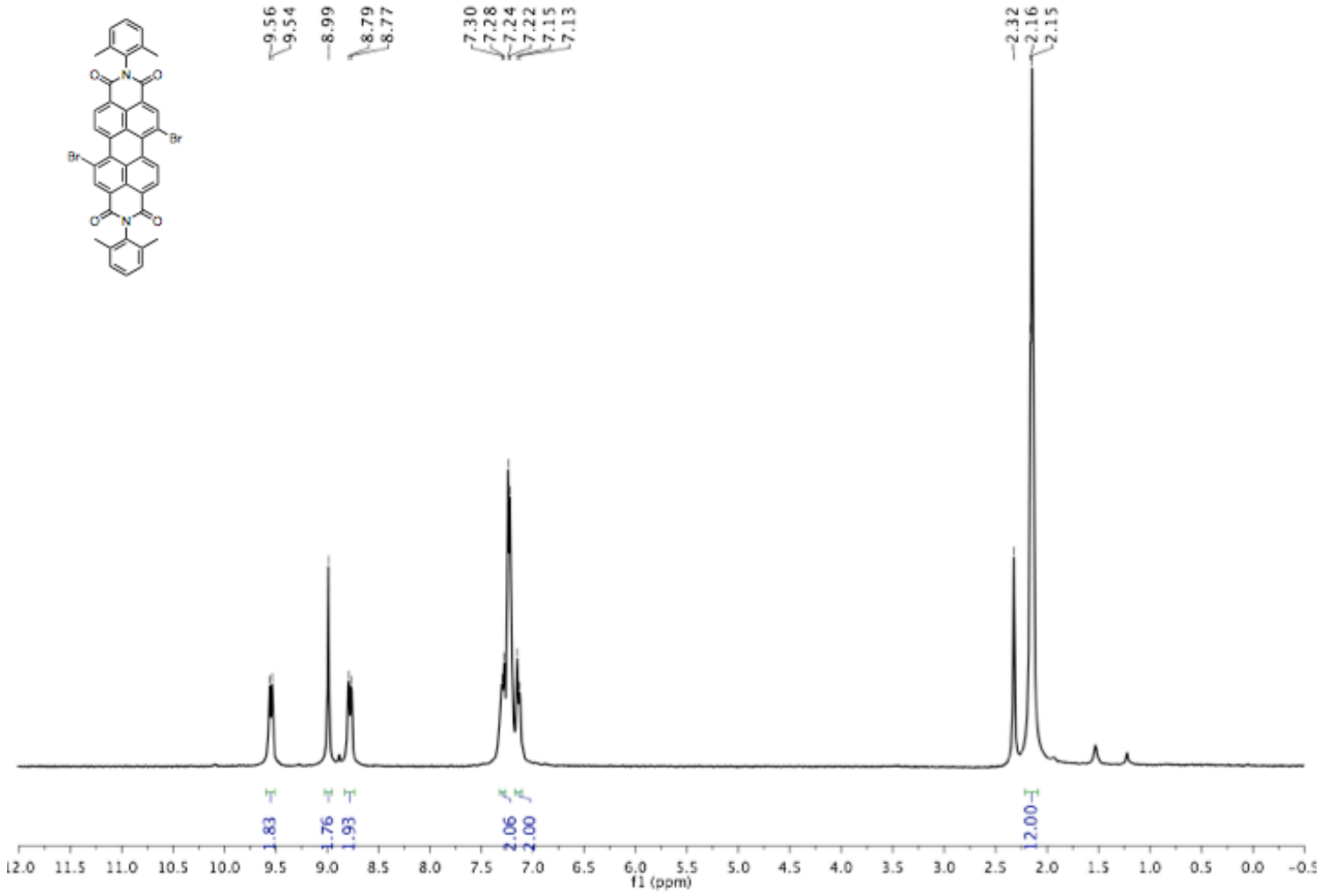

Appendix Figure 2.7. ^{1}H NMR of compound **5** in $CDCl_3$

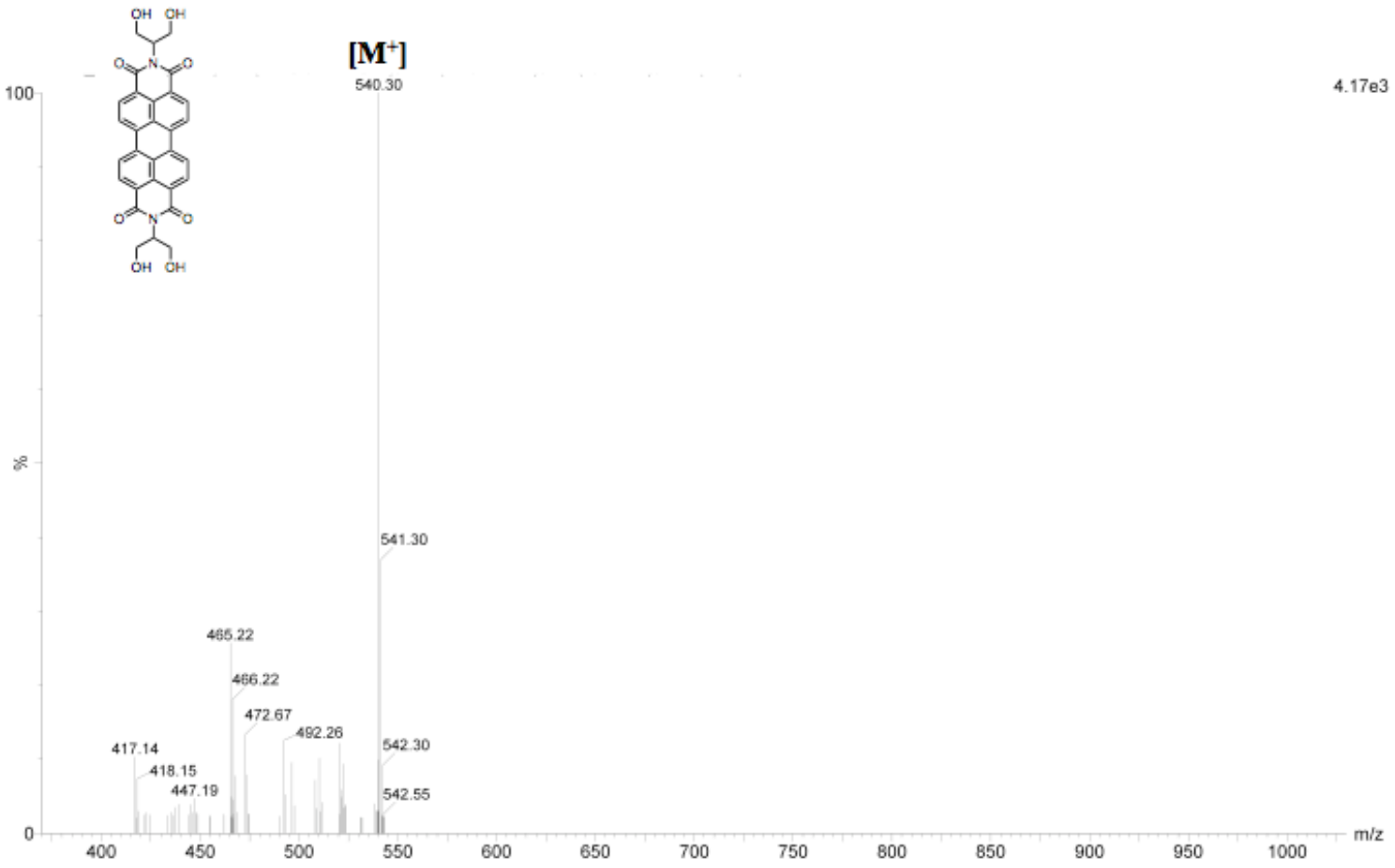

Appendix Figure 2.8. MALDI-TOF MS of compound **8**

REFERENCES

1. Langhals, H. *Helv. Chem. Acta.* **2005**, *88*, 1309-1343.

2. Würthner, F. *Pure Appl. Chem.* **2006**, *12*, 2341-2349.

3. Tomizaki, K.; Loewe, R.; Kirmaier, C.; Hindin, E.; Schwartz, J.; Bocian, D.; Holten, D.; Lindsey, J. *J. Org. Chem.* **2002**, *67*, 6519-6534.

4. Miller, M.; Lammi, R.; Prathapan, S.; Holten, D.; Lindsey, J. *J. Org. Chem.* **2000**, *65*, 6634-6649.

5. Neuteboom, E.; Meskers, S.; Van Hal, P.; Van Duren, J.; Meijer, E.; Janssen, R.; Dupin, H.; Pourtois, G.; Cornil, J.; Lazzaroni, R.; Brédas, J.; Beljonne, D. *J. Am. Chem. Soc*. **2003**, *125*, 8625-8638.

6. Gregg, B.; Cormier, R. *J. Am. Chem. Soc*. **2001**, *123*, 7959-7960.

7. Schmidt-Mende, L.; Fechtenkotter, A.; Müllen, K.; Moons, E.; Friend, R.; MacKenzie, J. *Science.* **2001**, *293*, 1119-1122.

8. Chopin, S.; Chaignon, F.; Blart, E.; Odobel, F. *J. Mater. Chem.* **2007**, *17*, 4139-4146.

9. Würthner, F.; Osswald, P.; Schmidt, R.; Kaiser, T., Manisikkamaki, H.; Konemann, M. *Org. Let*. **2006**, *8*, 3765-3768.

10. Bullock, J.; Carmiel, R.; Mickley, S.; Vura-Weis, J.; Wasielewski, M. *J. Am. Chem. Soc.* **2009**, *131*, 11919-11929.

11. Golubkov, G.; Weissman, H.; Shirman, E.; Wolf, S.; Pinkas, I.; Rybtchinski, B. *Angew. Chem. Int. Ed.* **2009**, *48*, 926-930.

12. El-Kaderi, H.; Hunt, J.; Mendoza-Cortés, J.; Côté, A.; Taylor, R.; O'Keeffe, M.; Yaghi, O. *Science*, **2007**, *316*, 268-272.

13. Silverstein, R.; Webster, F. *Spectroscopic Identification of Organic Compounds*. New York: John Wiley and Sons, **1998**.

14. Zhang, X.; Wu, Y.; Li, J.; Li, F.; Li, M. *Dyes and Pigments*, **2008**, *76*, 810-816.

15. Coventry, D.; Batsanov, A.; Goeta, A.; Howard, J.; Marder, T.; Pertuz, R. *Chem. Commun.* **2005**, 2172-2174.

16. Chen, H.; Hartwig, J. *Angew. Chem. Int. Ed.* **1999**, *38*, 3391-3395.

17. Ishiyama, M.; Murata, M.; Miyaura, N. *J. Org. Chem.* **1995**, *60*, 7508-7810.

18. Broutin, E.; Cerna, I.; Campaniello, M.; Leroux, F.; Colobert, F. *Org. Let.* **2004**, *6,* 4419-4422.

19. Kobayashi, N.; Kijima, M. *J. Mat. Chem.* **2008**, *18*, 1037-1045.

20. Rambo, B.; Lavigne, J. *Chem. Mater.* **2007**, *19*, 3732-3739.

21. Tilford, R.; Gemmill, W.; Loye, H.; Lavigne, J. *Chem. Mater.* **2006**, 18, 5296-5301.

22. Hunt, J.; Doonan, C.; LeVangie, J.; Côté, A.; Yaghi, O. *J. Am. Chem. Soc.* **2008**, *130*, 11872-11873.

23. Huang, W.; Yan, D.; Q, Lu; Huang, Y. *Eur. Poly. J.* **2003**, *39*, 1099-1104.

24. Rohr, U.; Kohl, C.; Müllen, K.; Craats, A.; Warman, J. *J. Mat. Chem.* **2001**, *11*, 1789-1799.

25. Würthner, F.; Stephanenko, V.; Chen, Z.; Saha-Möller, C.; Kocher, N.; Stalke, D. *J. Org. Chem.* **2004**, *69*, 7933-7939.

CHAPTER 3:

Oligothiophenes for *p*-Type Organic Semiconducting COFs

3.1. Abstract

The synthesis of **2**, **3a**, and **6** boronic acid derivatives was obtained by Suzuki coupling and lithiation techniques in moderate yields characterized by MALDI, FT-IR, and/or multinuclear NMR spectroscopy. These compounds are the most promising candidates to form **COF-1T**, **COF-2T**, and **COF-3TN**.

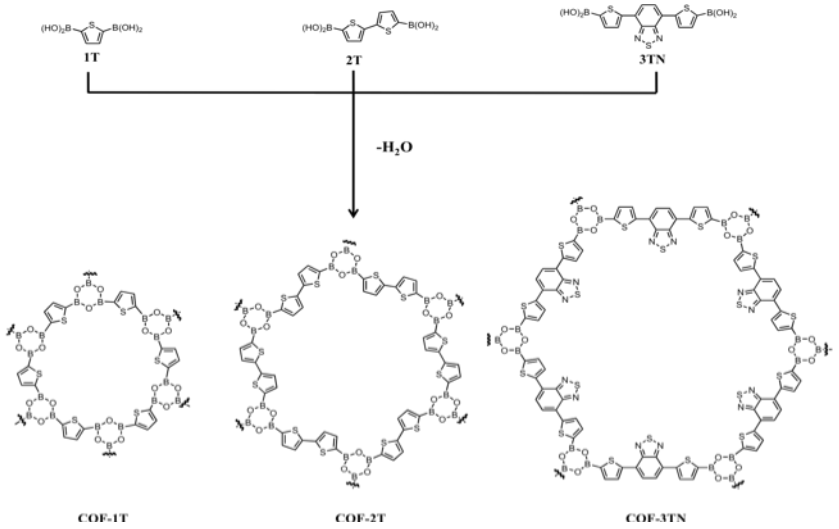

Figure 3.1. Proposed boroxine thiophene COFs by self-condensation.

3.2. Introduction

Oligothiophenes have received remarkable attention as widely used lightweight π-conjugated materials in light-emitting diodes (OLED/ PLEDs)[1-2], field-effect transistors (FET)[3-4], and photovoltaic cells[5] because of their ability to acquire positive holes and their rich electron environment[6-7]. More important, homocoupling of thiophenes by transition-metal catalysts, such as Stille and Suzuki coupling, offers a practical and simple way to afford oligothiophenes in high yields and as well-defined

structures[8]. For these reasons, oligothiophenes are attractive candidates to form light-harvesting COFs.

In this chapter, the syntheses of **1T**, **2T**, and **3TN** boronic acid derivatives were attempted as building blocks for the proposed boroxine COFs: **COF-1T**, **COF-2T**, and **COF-3TN** (Figure 3.1).

3.3. Synthesis of 1T boronic acid to form COF-1T

In an attempt to synthesize **COF-1T**, the model compound **1** was created following literature procedures[9-10] for the synthesis of **1**, where **1** is known as the model compound for **COF-1** by, Yaghi and colleagues[10]. To test the reliability of Rambo and colleagues' method[9], the synthesis of **1** and **2** was prepared in our lab (Figure 3.2). The characterization of analytically pure **1** was difficult to ascertain by ^{1}H, ^{13}C, and ^{11}B NMR spectroscopy because of the acidity of $CDCl_3$, which allows the anhydride to establish equilibrium with its semianhydride and free boronic acid form. This observation is consistent with results reported by Rambo and colleagues[9]. A reliable method for characterization of **1** is based on FT-IR spectroscopy, in which the disappearance of the OH stretch at 3200-3400 cm^{-1} and appearance of a broad B-O stretch at 1300-1350 cm^{-1} indicate boroxine ring formation[10]. Based on FT-IR analysis, **1** was synthesized successfully with a spectral signature in agreement with Côté and colleagues[9] showing evidence of B-O linkage at 1333 and 1304 cm^{-1}, respectively (Figure 3.3). In addition, small sp^2 C-H stretches of the phenyl ring at 3078 and 3052 cm^{-1} are observed, values similar to those reported in the literature[10].

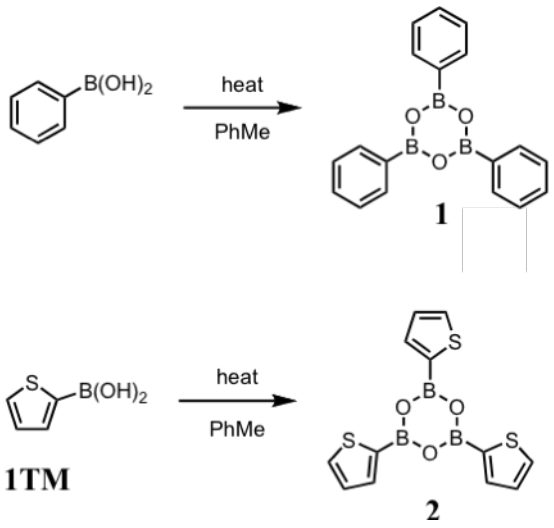

Figure 3.2. Thermal dehydration of phenyl and thiophene boronic acids to boroxine **1** and **2**.

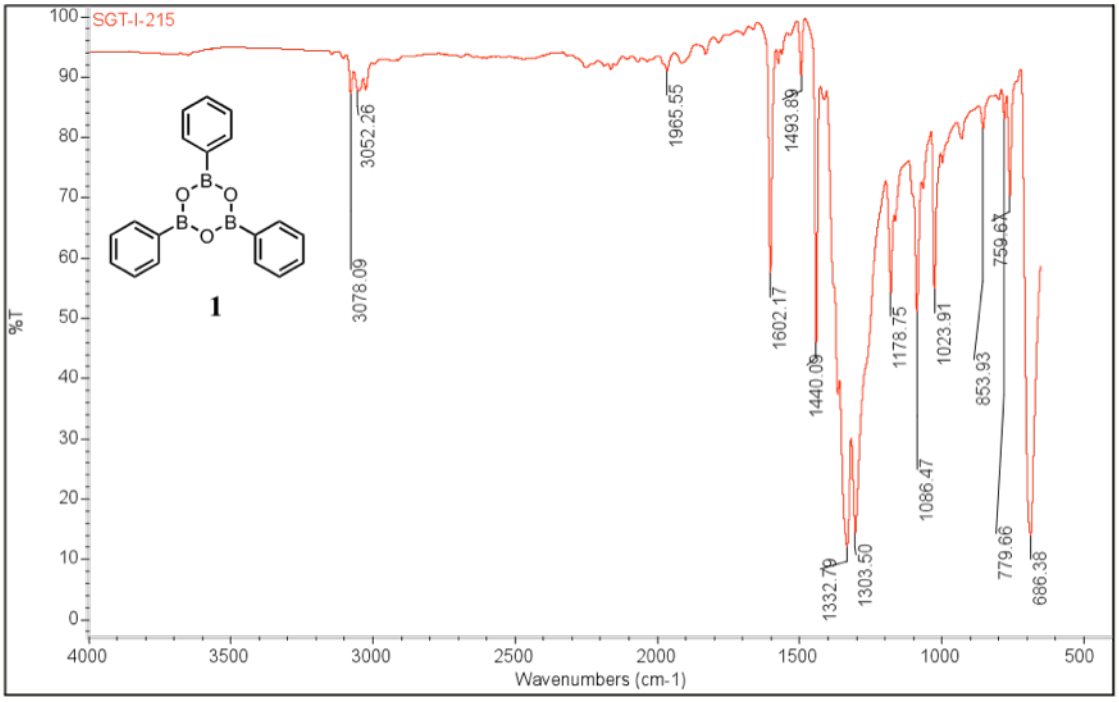

Figure 3.3. FT-IR spectra of **1** by thermal dehydration of phenyl boronic acid.

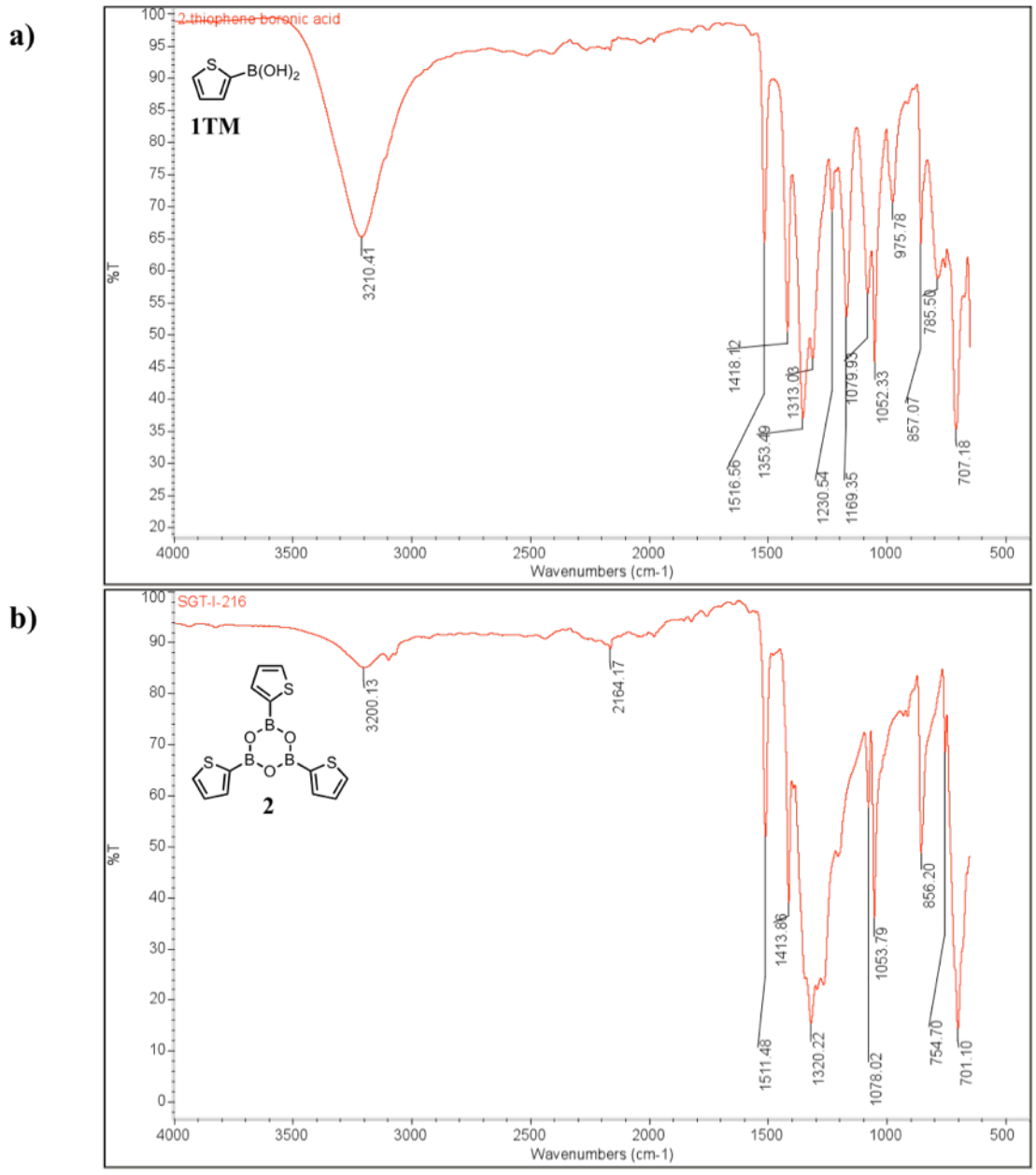

Figure 3.4. (a) FT-IR spectra of 2-thiophene boronic acid (**1TM**); (b) FT-IR spectra of **2**.

By the same token, **2** was characterized by FT-IR and multinuclear NMR .analysis. Based on ^{1}H, ^{13}C, and ^{11}B NMR spectroscopy, very little difference in chemical signals is seen compared with 2-thiophene boronic acid[11] (**1TM**), making it difficult to determine whether **2** was actually formed. Evidence for **2** is observed by

FT-IR analysis, with a significant diminishing of the OH peak at 3200 cm^{-1} (Figure 3.4b) compared with 3210 cm^{-1} of **1TM** (Figure 3.4a). In addition, the B-O stretch of **2** at 1320 cm^{-1} differs significantly from the B-O stretch of **1TM** at 1353 and 1313 cm^{-1}, affirming successful thermal dehydration of **1TM** to **2** (Figure 3.4).

In summary, **1** and **2** were synthesized successfully, suggesting that **2** can be used as the model compound for **COF-1T**.

3.4. Synthesis of 2T boronic acid to form COF-2T

The design of **COF-2T** requires the synthesis of **3a**, which was obtained by deprotonation of the α-protons of bithiophene at C-5 and C-5′ by *n*-BuLi and triisopropyl borate addition after an acidic workup (Figure 3.5).

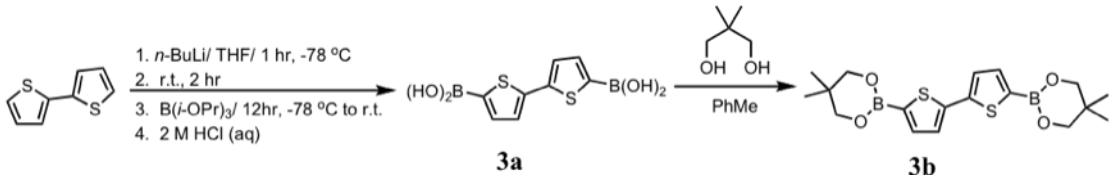

Figure 3.5. Borylation of bithiophene to **3a** and its derivatization to **3b**.

The success of **3a** is evidenced by the presence of two doublets at 7.64 and 7.37 ppm, which reflects the absence of doublet of doublet signals for H-5 and H-5′ protons in ^{1}H NMR, thus demonstrating that boryl groups are attached at these positions. The three signals at 143.6, 137.4, and 125.9 ppm in the aromatic region of ^{13}C NMR reflect the symmetry of **3a**, and correspond to the C-2 and C-2′; C-3 and C-3′; and C-4 and C-4′ positions, respectively, whereas the signals for C-5 and C-5′ are not visible as a result of carbon-boron coupling. In addition, the ^{11}B NMR spectrum shows a signal at 23.2 ppm, further confirming the structure of **3a**. Another structural characteristic of **3a** is seen by FT-IR spectroscopy, which reveals a distinct OH stretch at 3215 cm^{-1} and the presence of a broad B-O stretch at 1330 cm^{-1} (Figure 3.6).

Finally, MALDI-TOF MS analysis of **3a** also includes product formation after derivatization by neopentyl glycol to **3b**, at a *m/z* of 394.4. This technique is necessary for characterization of boronic acids because of their partial dehydration and cyclization to boroxines in the GC-MS inlet if not protected[12].

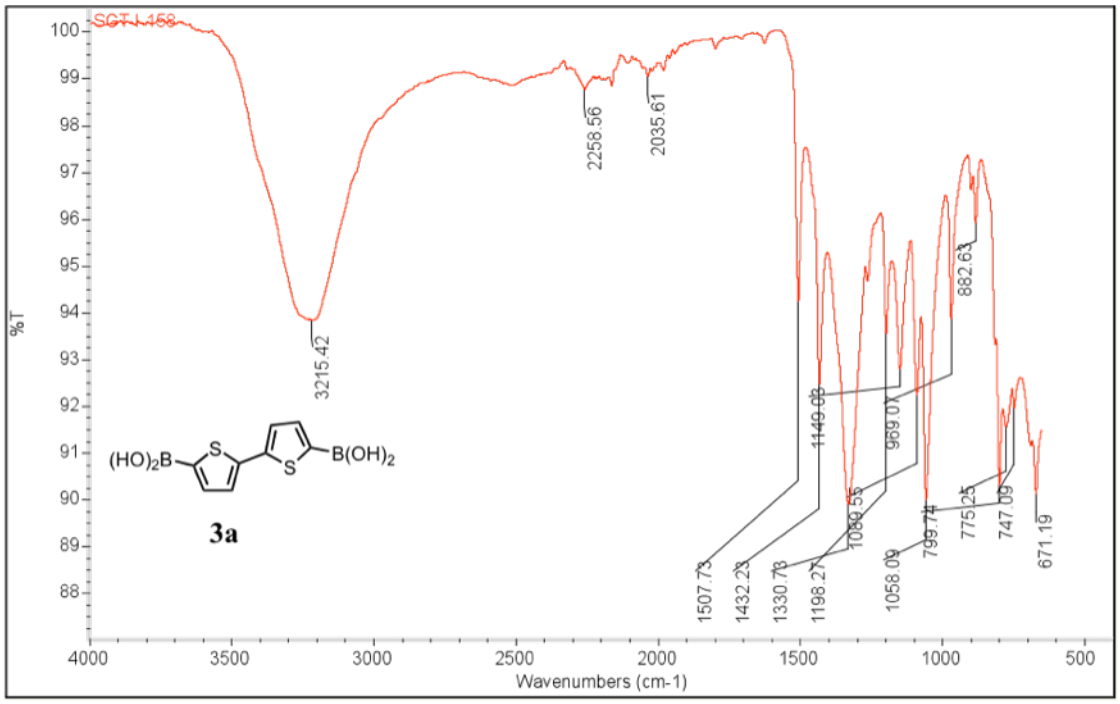

Figure 3.6. FT-IR spectra of **3a** illustrating boronic acid formation.

Finally, one should take into account the stability of **3a** because of its susceptibility to atmospheric oxidation to a phenol derivative[13] at room temperature. Care was taken to store **3a** at 0 ºC under nitrogen, and it was dried for only 1 hr to prevent its cyclic dehydration to boroxine[13]. An interesting phenomenon associated with **3a** acetone solutions was observed in which the color of the solutions changed from clear to deep blue after 24 hr exposure to air, which may suggest that **3a** is not stable in solutions for prolonged periods at room temperature. To confirm this observation would require analysis of both solutions by UV-Vis spectroscopy to

identify shifts in absorption wavelengths of **3a** and possible byproducts. In sum, based on spectroscopic analysis, structural confirmation of **3a** was indeed successful.

Based on the success of **3a** by *n*-BuLi deprotonation chemistry, an alternate facile method toward **3a** as a boronic ester (**3c**) should be considered using Miyaura borylation coupling because of its economical reaction conditions and tolerance to various functional groups (Figure 3.7). Thus, **4** was synthesized by NBS bromination in excellent yield, with a ^{1}H and ^{13}C NMR spectra, in agreement with the literature[14]. Preliminary work by palladium borylation coupling to **3c** was carried out in our laboratory, and further investigation of its optimization should be considered.

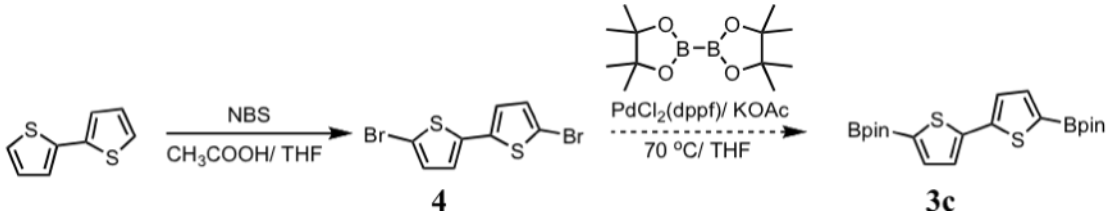

Figure 3.7. Alternate route to **3a** as a boronic ester (**3c**) by Miyaura borylation coupling.

3.5. Synthesis of 3TN to form COF-3TN

As technologies evolve to form better and more efficient organic semiconducting materials, there is a need to optimize the current technologies for better performance. This can be achieved by using oligothiophenes with different functional groups, resulting in enhanced electron delocalization within the π system as a consequence of an altered HOMO-LUMO bandgap. Specifically, 2,1,3-benzothiadiazole is an electron-deficient monomer known for its low bandgap and high charge carrier mobility, conveniently allowing optical absorption at longer wavelengths toward infrared light[15]. Using this concept, **5** was synthesized following a modified procedure by Neto and colleagues[16] in 53% yield as a yellow solid. The

synthesis of **6** was carried out by Suzuki coupling between **5** and **1TM** for 16 hr and purified by column chromatography (4:1 petroleum ether: $CHCl_3$), and was followed by recrystallization from $CHCl_3$-acetone to afford a bright orange solid in 4% yield (Figure 3.8).

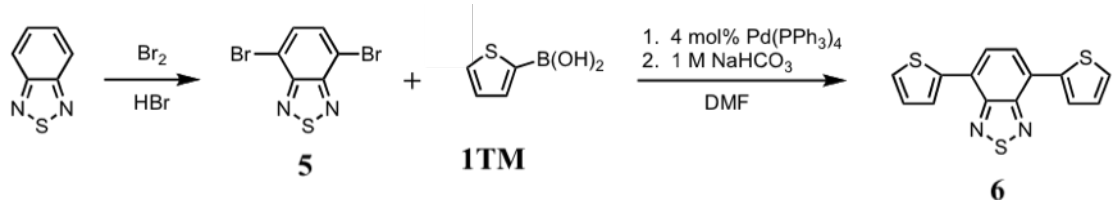

Figure 3.8. Synthesis of **5** and **6** by bromination and Suzuki coupling.

The observed resonance of the phenyl proton at 7.86 ppm for **6** compared with **5** at 7.71 ppm by ^{1}H NMR and a *m/z* of 299.6 by MALDI-TOF MS indicates that the Suzuki coupling with **1TM** was a success. To improve the synthesis of **6**, four equivalents of **1TM** were used, increasing the yield to 10% (0.0843 g). The extremely low yields are attributed to oligomer mixtures that were challenging to separate by column chromatography (4:1 petroleum ether: $CHCl_3$) as a result of very close R_f values by TLC. In sum, the synthesis of **6** was successful, and lithiation-borylation at C-2′ and C-2′′ positions would be the next step to obtain **3TN** boronic acid using the synthetic methodologies described in 3.4.

3.6. Future work and conclusions

Compounds **2**, **3a**, and **6** are the most likely candidates so far for the creation of **COF-1T**, **COF-2T**, and **COF-3TN** using the methodologies described in this chapter. Besides the proposed *n*-type or *p*-type COFs discussed in chapters 2 and 3, one should take into consideration the design of a hybrid *n*-type-*p*-type COF as a brand-new semiconducting material containing both PDI (*n*-type) and oligothiophene

(*p*-type) building blocks. Efforts to form an *n*-type–*p*-type hybrid material are already well established in the literature, where PDI-oligothiophene-PDI triad linkages by Suzuki and Negishi coupling are being investigated as potential materials for organic solar cells with bandgaps as low as 2.11 eV[17-18]. In addition, this triad displays good electron transporting properties, and exhibits energy conversions up to 0.5% under a simulated terrestrial sun spectrum[6,18] (Figure 3.9). Although innovative, the creation of a hybrid semiconducting COF is indeed complex, and attempts to engineer its properties as a crystalline material would require significant synthetic protocol.

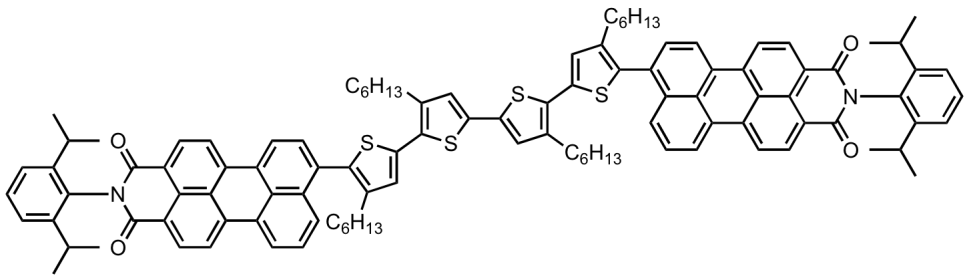

Figure 3.9. Example of hybrid *n*-type and *p*-type triad consisting of PDI and oligothiophenes.

In sum, the synthesis of PDI and oligothiophene boronic acids as photoactive monomers and the study of electronic properties in a COF material would serve as breakthroughs in current COF technologies. Perhaps in the near future photoactive COFs can serve as another alternative for well-ordered semiconducting materials.

3.7. Experimental section

3.7.1 General considerations

All manipulations were carried out under a nitrogen atmosphere using flame-dried glassware following standard vacuum line and Schlenk techniques. All compounds unless otherwise stated were purchased from Sigma Aldrich and Alfa Aesar and used as received. Methanol, tetrahydrofuran, N,N-dimethylformamide, and

toluene were obtained from a custom-built alumina column solvent purification system. ^{1}H, ^{13}C, and ^{11}B NMR were obtained on a 300 MHz Bruker Avance NMR spectrometer using $CDCl_3$, CD_2Cl_2, or acetone-*d6* as solvent. FT-IR measurements were taken on a Nicolet iS10 FT-IR spectrometer from Thermo Fisher Scientific. MALDI-TOF measurements were taken on a Waters MALDI Micro MX spectrometer on positive-mode ionization using dithranol as a matrix.

Phenylboronic anhydride (1): Compound **1** was synthesized following literature procedures with slight modifications[9]. To a 100 mL round-bottom flask equipped with a magnetic stirbar and nitrogen inlet was added phenylboronic acid (0.500 g, 4.101 mmol) in toluene (21 mL). The reaction mixture was heated at reflux for 90 min with a Dean-Stark trap filled half full with 3Å molecular sieves. The reaction mixture was concentrated under reduced pressure to afford **1** as a white solid (0.394 g, 31%). FT-IR (neat): 3078, 3052, 1966, 1602, 1494, 1440, 1332, 1303, 1179, 1086, 1024, 854, 780, 760, 686 cm^{-1}; ^{1}H NMR (300 MHz, $CDCl_3$): ∂ 8.25 (d, J = 6.75 Hz, 4H), 7.62 (t, J =7.57 Hz, 2H) 7.53 (t, J =7.57 Hz, 4H); ^{13}C NMR (75 MHz, $CDCl_3$): ∂ 136.4, 133.4, 128.7; ^{11}B NMR (96 MHz, $CDCl_3$): ∂ 32.5.

2-thiopheneboronic anhydride (2): Compound **2** was synthesized following the same procedure as **1** using 2-thiophene boronic acid (0.500 g, 3.907 mmol) in toluene (20 mL) to afford **2** as a white solid (0.337 g, 28%). FT-IR (neat): 3200, 2164, 1512, 1414, 1320, 1078, 1054, 856, 755, 701 cm^{-1}; ^{1}H NMR (300 MHz, $CDCl_3$): ∂ 8.03 (d, J = 3.11 Hz, 3H), 7.80 (d, J =4.62 Hz, 3H) 7.33 (t, J =4.24 Hz, 3H); ^{13}C NMR (75 MHz, $CDCl_3$): ∂ 139.7, 135.0, 128.8; ^{11}B NMR (96 MHz, $CDCl_3$): ∂ 30.3.

2,2´-bithiophene-5,5´-diboronic acid (3): Compound **3** was synthesized following literature procedures with slight modifications[8]. To a 250 mL three-neck round-

bottom flask equipped with magnetic stirbar, rubber septa, and nitrogen inlet was added 2,2′-bithiophene (1.000 g, 6.015 mmol) in THF (20 mL) at -78 °C and stirred for 2 hr, after which *n*-BuLi (2.5 M in hexane, 5.48 mL, 13.71 mmol) was added dropwise to form a light green solution that was stirred for 1 hr at -78 °C. The reaction mixture was then allowed to stir for 2 hr at r.t. and cooled back to -78 °C, which was stirred for an additional 15 min. Triisopropylborate (5.656 g, 30.073 mmol) in THF (15 mL) was added dropwise to the reaction mixture, and the milky white solution was stirred at -78 °C for 1 hr and then warmed slowly to r.t. After stirring overnight, 2 N HCl (41 mL) was added to the reaction mixture and stirred vigorously for 15 min. The organic (THF) layer was separated and the aqueous layer was extracted with Et_2O (2 x 50 mL), dried with $MgSO_4$, concentrated under reduced pressure and dried for 1 hr under high vacuum to afford **3** as a light green solid (0.928 g, 61%) that was stored at 0 °C. FT-IR (neat): 3215, 2259, 1507, 1432, 1330, 1198, 1149, 1089, 1058, 969, 882, 799, 775, 747, 671 cm^{-1}; ^1H NMR (300 MHz, acetone-*d6*): ∂ 7.62 (d, J = 3.86 Hz, 2H), 7.36 (d, J = 3.60 Hz, 2H); ^{13}C NMR (75 MHz, acetone-*d6*): 143.6, 137.4, 125.9; ^{11}B NMR (96 MHz, acetone-*d6*) ∂ 23.2. MALDI-TOF MS was obtained as **3b** by capping the boronic acid with neopentyl glycol. MALDI-TOF calcd for $[C_{18}H_{24}B_2O_4S_2]^+$ 390.13, found 394.41.

5,5′-dibromo-2,2′-bithiophene (4): Compound **4** was synthesized following a modified procedure by Lightowler et al[14]. To a 50 mL round-bottom flask equipped with magnetic stirbar was added 2,2′-bithiophene (1.000 g, 6.015 mmol) in 1:1 THF: acetic acid (8 mL) and allowed to stir for 10 min. Then, NBS (2.142 g, 12.029 mmol) was added in portions to the reaction mixture and allowed to stir for 2 hr under light protection at r.t. The precipitate was filtered, washed with H_2O (2 x 20 mL) and dried under high vacuum to afford **4** as white needles (1.61 g, 83%). ^1H NMR (300 MHz,

CD_2Cl_2): ∂ 7.00 (d, J = 3.51 Hz, 2H); 6.89 (d, J = 3.71 Hz, 2H); ^{13}C NMR (75 MHz, CD_2Cl_2): 138.4, 131.4, 124.9, 112.0.

4,7-dibromo-2,1,3-benzothiadiazole (5): Compound **5** was synthesized following a modified procedure by Neto et al[16]. To a 250 mL three-neck round-bottom flask equipped with magnetic stirbar, condenser, nitrogen inlet, vent needle, and addition funnel was added 2,1,3-benzothiadiazole (2.720 g, 19.975 mmol) in 47% aqueous HBr (40 mL) that was allowed to reflux under stirring for 1 hr to afford a bright orange solution. Then, bromine (6.384 g, 39.950 mmol) was added dropwise in 15 min intervals over the course of 1 hr. The resulting reaction mixture was allowed to reflux for an additional 2 hr to yield a yellow needle-like precipitate that was filtered, and then washed thoroughly with H_2O (2 x 50 mL) and 0.5 M $NaHSO_3$ (3 x 50 mL), which was recrystallized from EtOAc to afford **5** as yellow needles (3.08 g, 53%). ^1H NMR (300 MHz, $CDCl_3$): ∂ 7.71 (s, 2H).

3,4-(2,1,3-benzothiadiazole)-2,2´:5´,2´´-terthiophene (6): To a 100 mL three-neck round-bottom flask equipped with magnetic stirbar, condenser, nitrogen inlet, and rubber septa was added **5** (0.800 g, 1.840 mmol) in DMF (25 mL) under stirring; then $[Pd(PPh_3)_4]$ (0.126 g, 0.109 mmol) was added to the reaction mixture and stirred for 10 min forming a red solution. Then, 2-thiopheneboronic acid (0.836 g, 6.531 mmol) and 1 M $NaHCO_3$ (1.2 mL) was added to the reaction mixture, which was refluxed overnight under exclusion of light. The deep red solution was poured into H_2O (75 mL) to afford a bright opaque orange solution that was extracted with Et_2O (3 x 75 mL), dried with $MgSO_4$ and concentrated under reduced pressure to afford a crude red oil that was purified by column chromatography (4:1 petroleum ether: $CHCl_3$). The orange semisolid was further purified by dissolving the crude in a minimal amount of

$CHCl_3$ and carefully layering with 2 mL acetone that was exposed to air overnight. The concentrated acetone solution, when cooled at 0 ºC, was filtered and washed with cold acetone (2 x 5 mL) to afford **6** as bright orange needles (0.028 mg, 4%). ^{1}H NMR (300 MHz, $CDCl_3$): ∂ 8.11 (d, J = 3.64 Hz, 2H); 7.86, (s, 2H), 7.45 (d, J = 4.76 Hz, 2H); 7.21 (t, J = 4.14 Hz, 2H); MALDI-TOF calcd for $[C_{14}H_8N_2S_3]^+$: 299.98, found 299.6.

APPENDIX

The following section includes MALDI, ^{1}H, ^{13}C, and ^{11}B NMR spectra for characterization of compounds **1-6**. All spectra were recorded based on considerations mentioned in section 3.7.

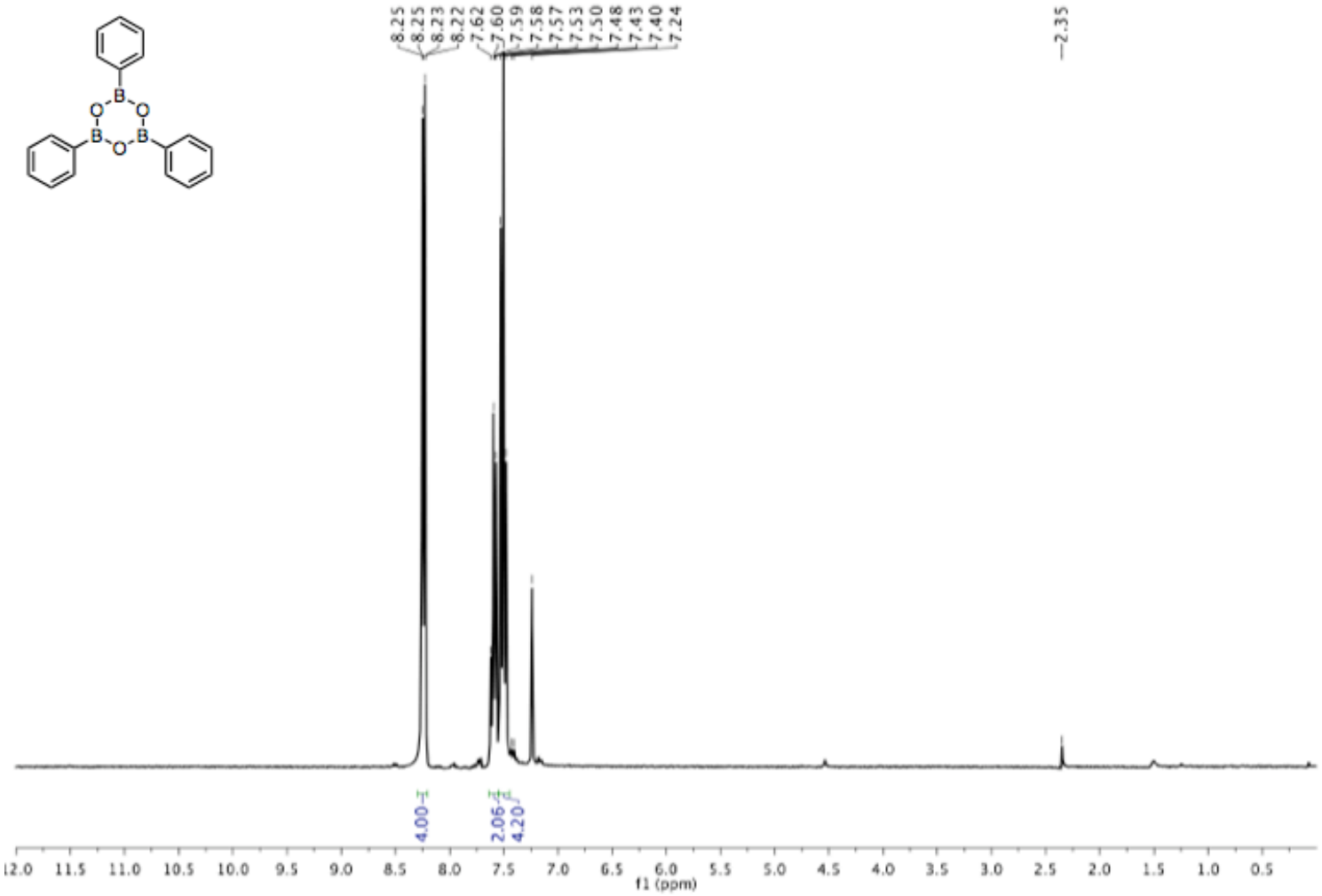

Appendix Figure 3.1. ^{1}H NMR of compound **1** in $CDCl_3$

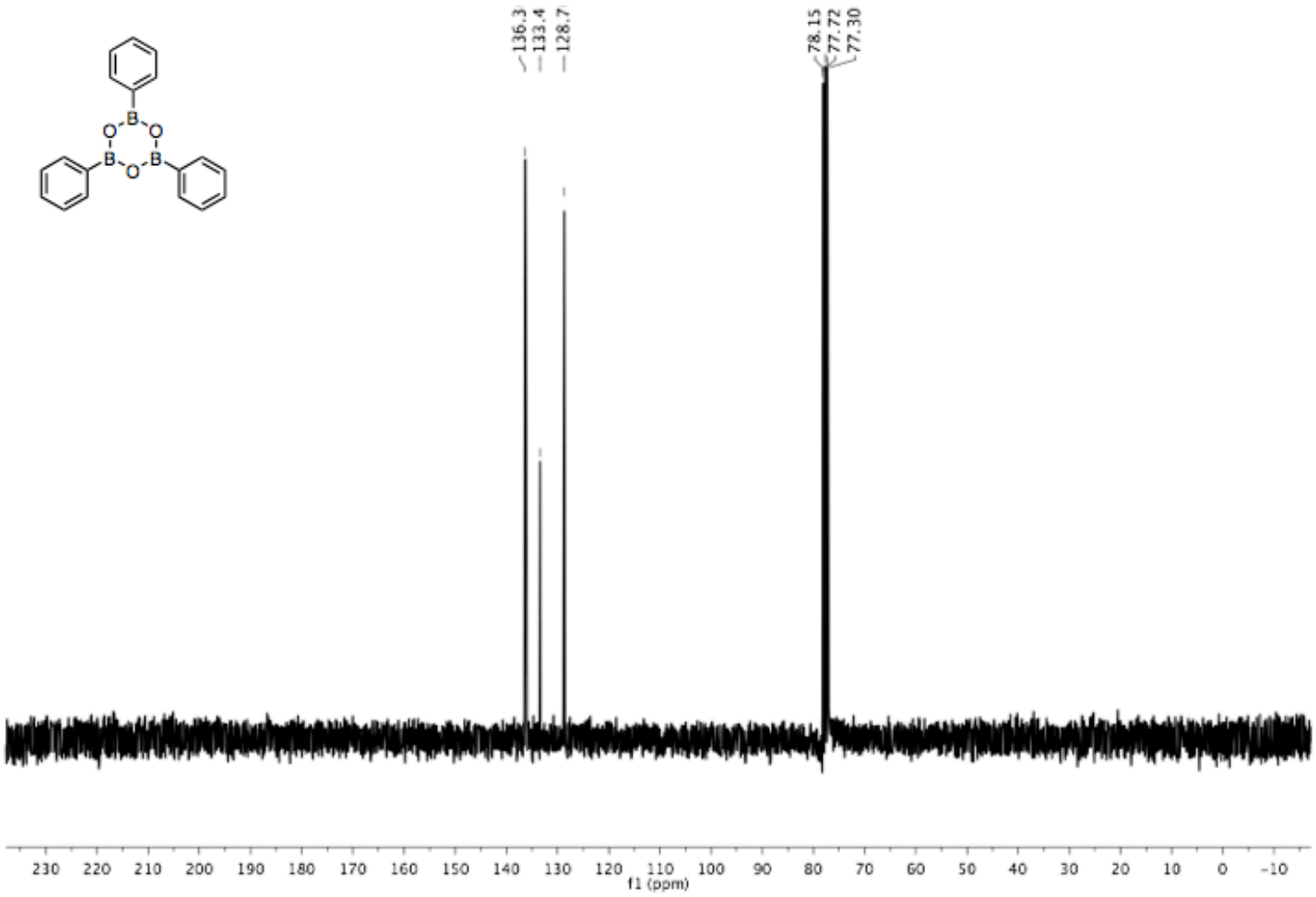

Appendix Figure 3.2. ^{13}C NMR of compound **1** in $CDCl_3$

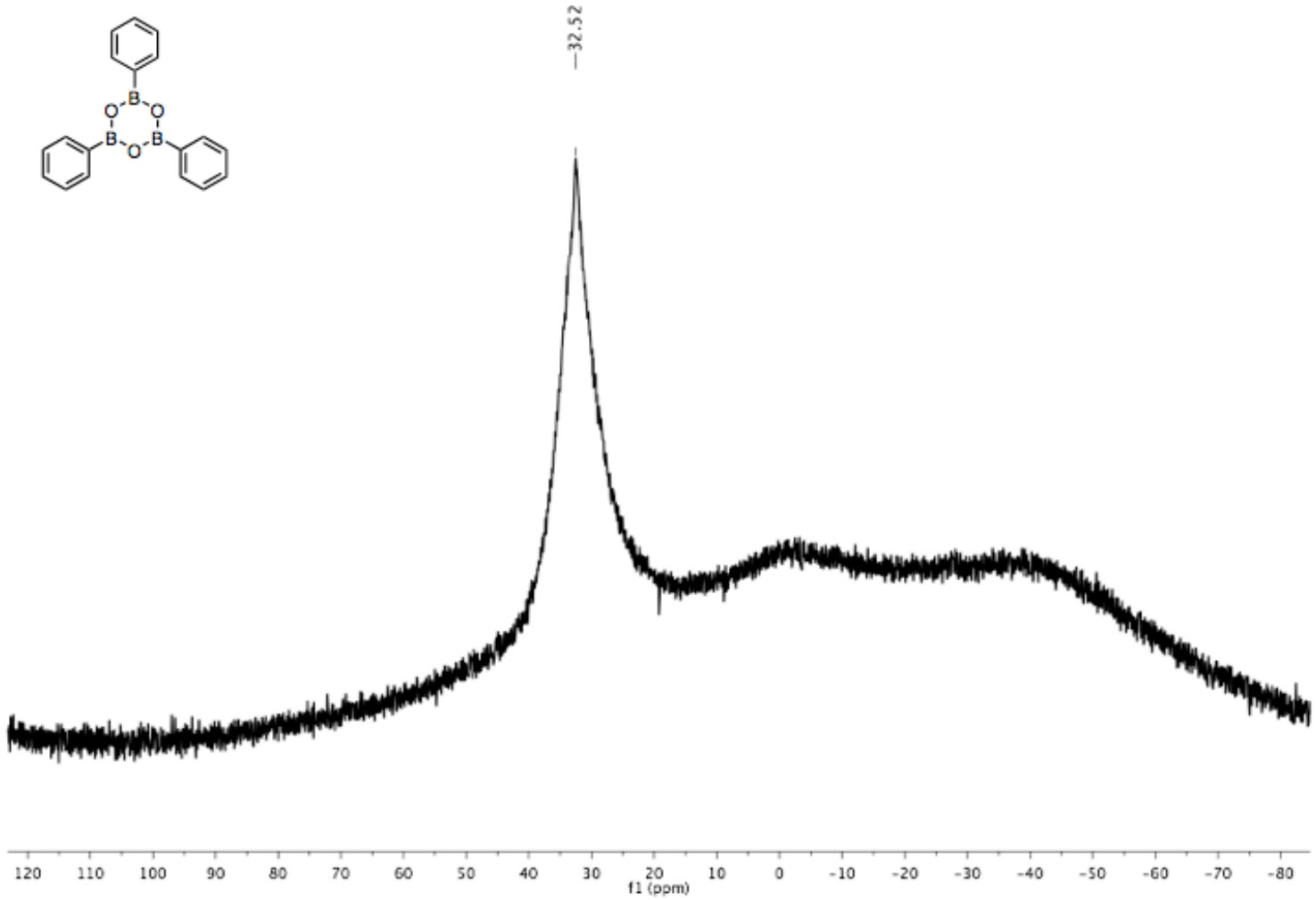

Appendix Figure 3.3. ^{11}B NMR of compound **1** in $CDCl_3$

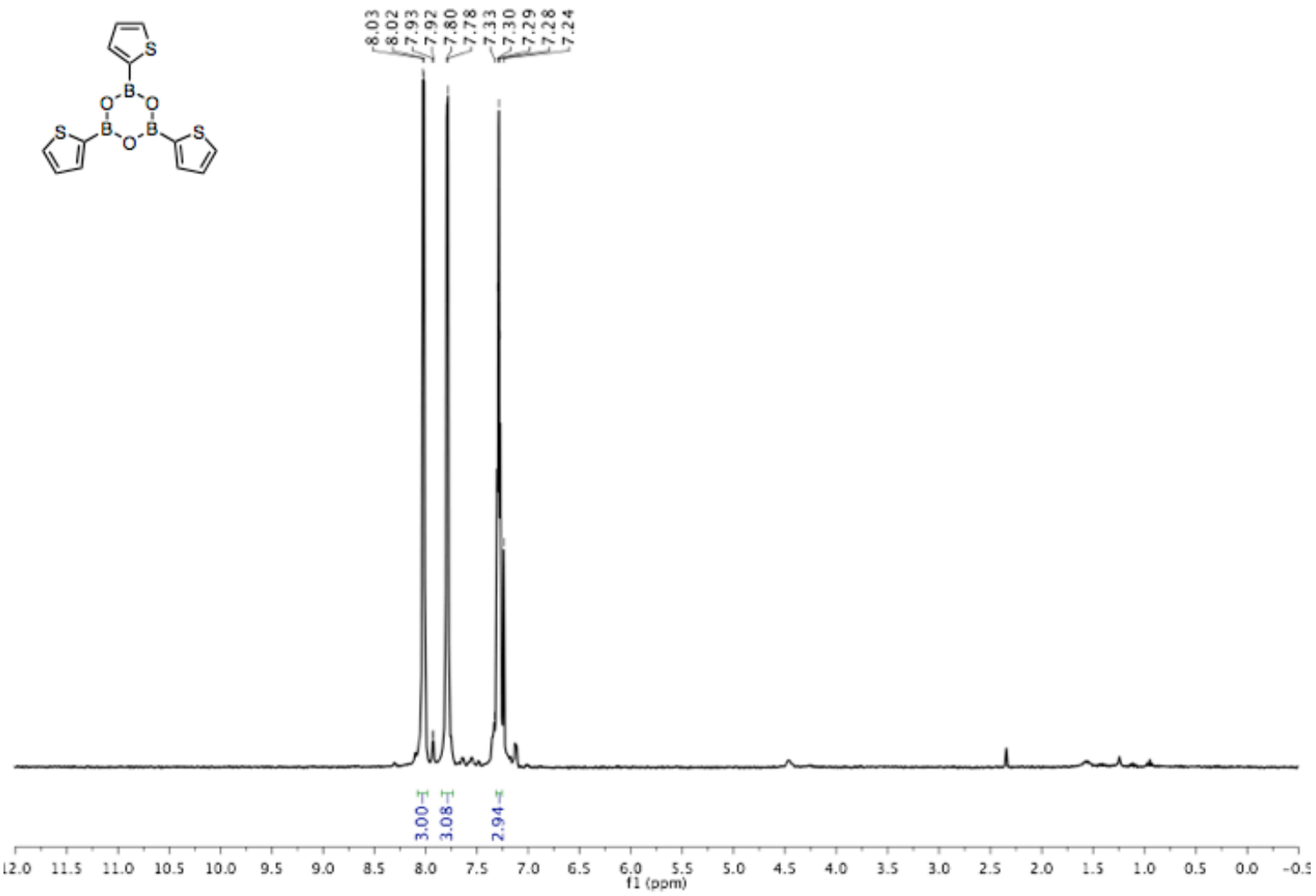

Appendix Figure 3.4. ^{1}H NMR of compound **2** in $CDCl_3$

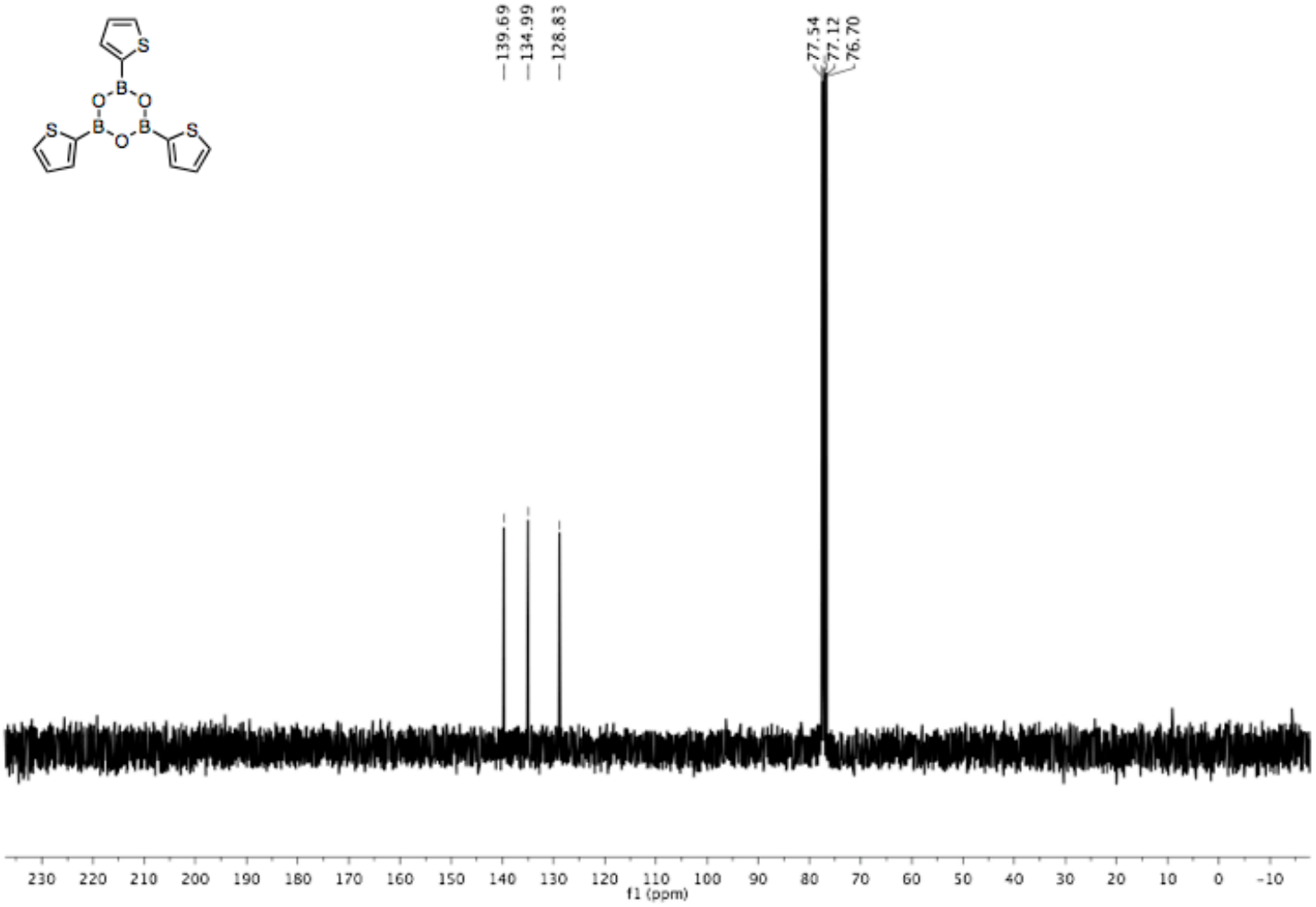

Appendix Figure 3.5. ^{13}C NMR of compound **2** in $CDCl_3$

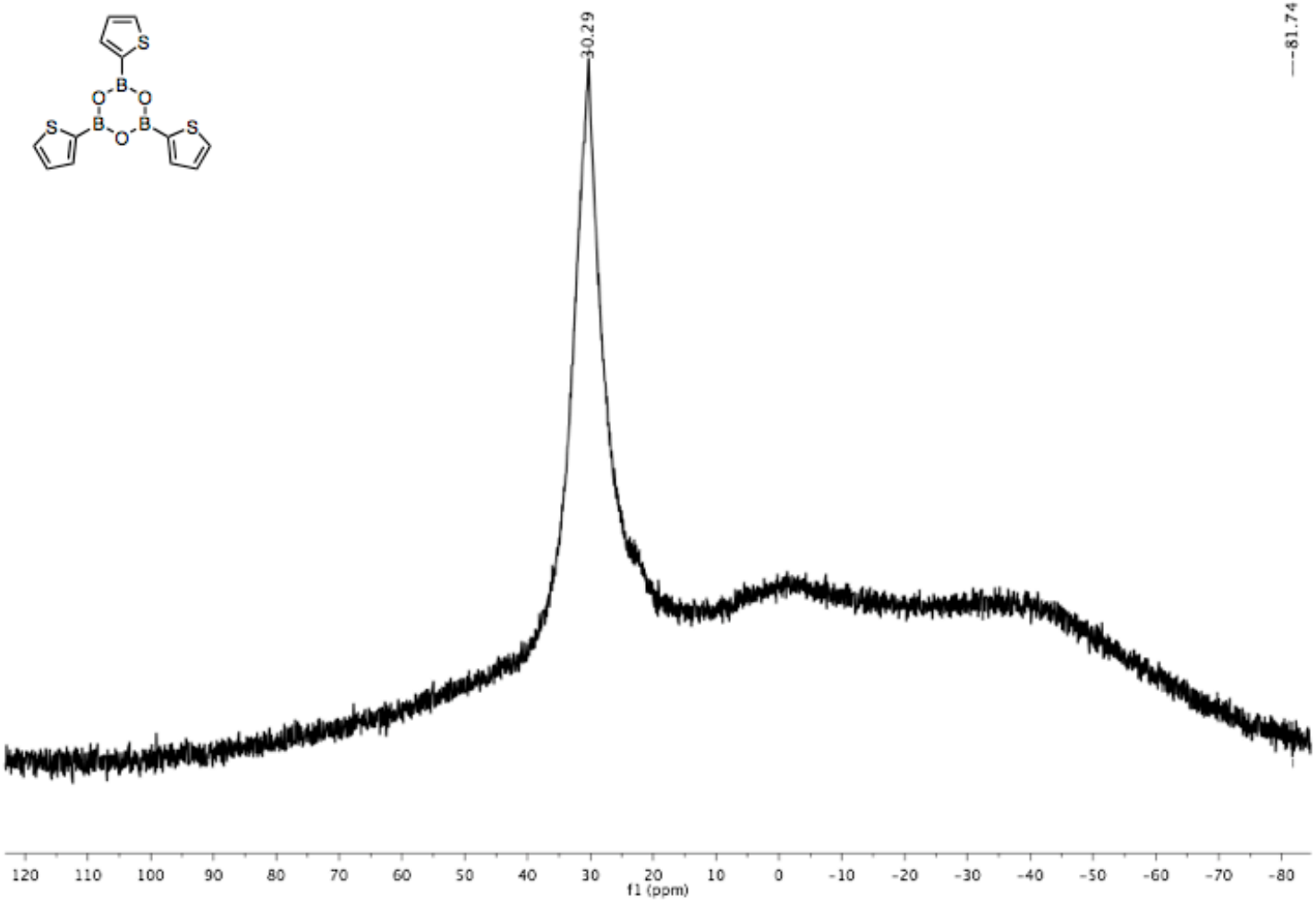

Appendix Figure 3.6. ^{11}B NMR of compound **2** in $CDCl_3$

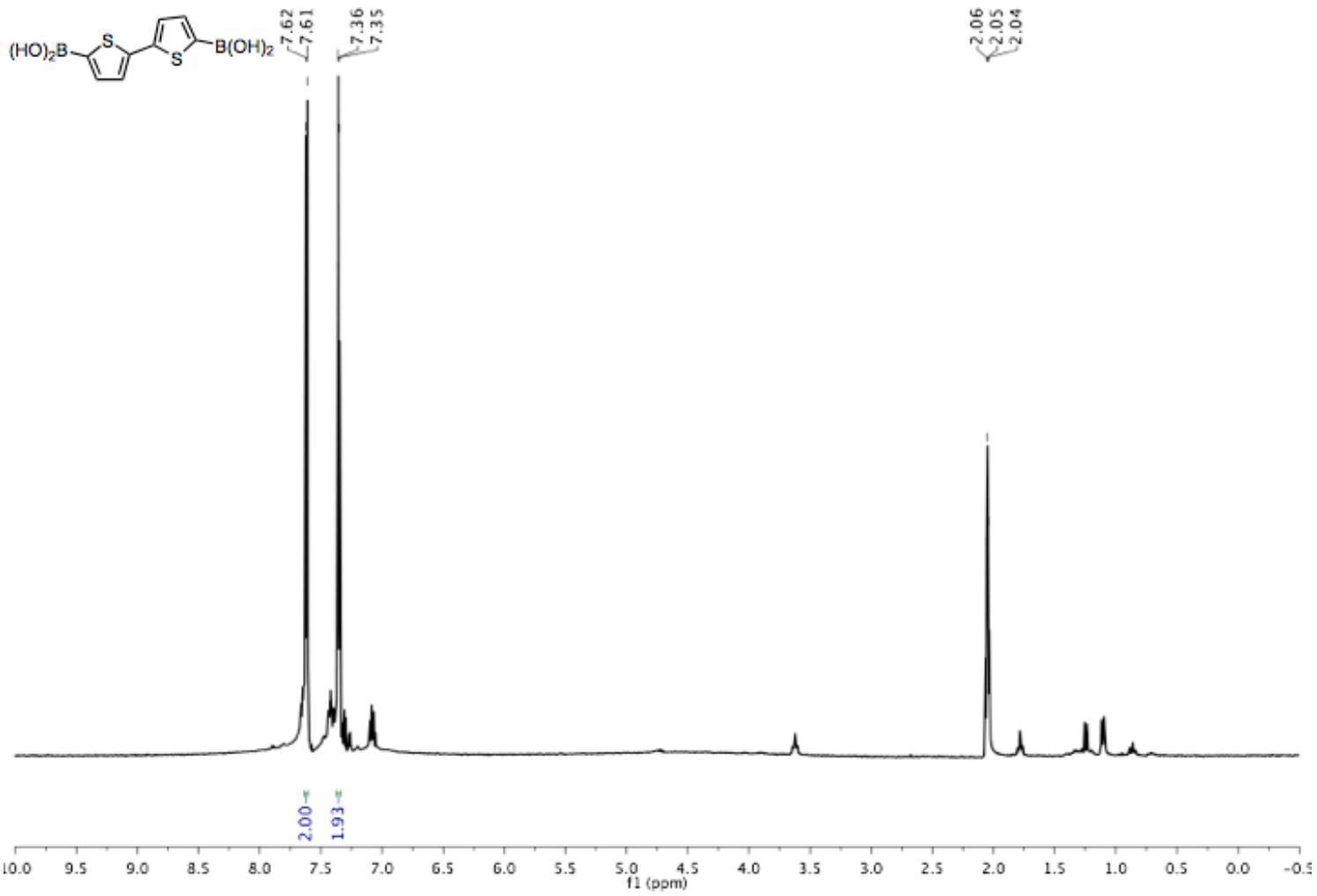

Appendix Figure 3.7. ^{1}H NMR of compound **3** in $CDCl_3$

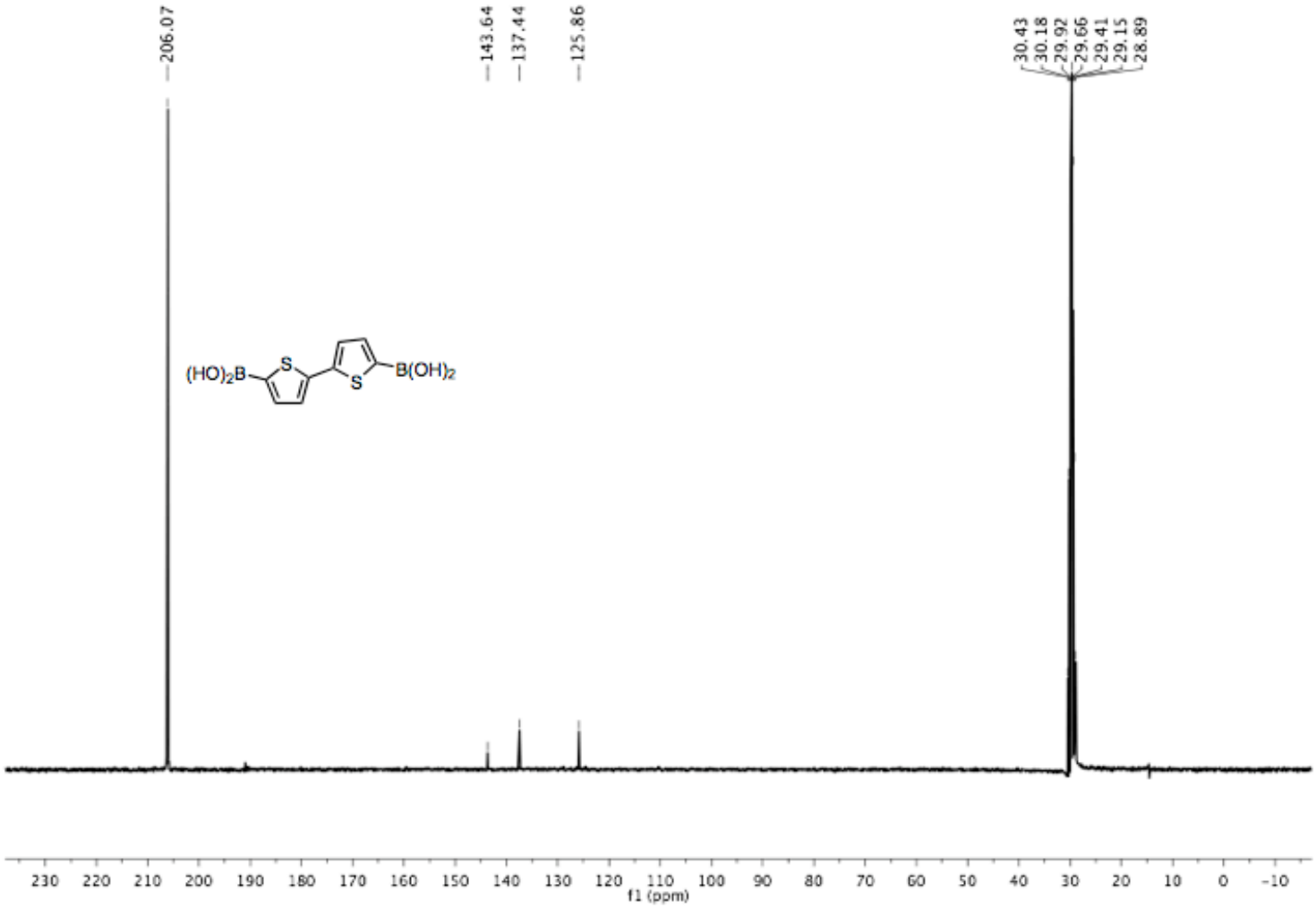

Appendix Figure 3.8. ^{13}C NMR of compound **3** in $CDCl_3$

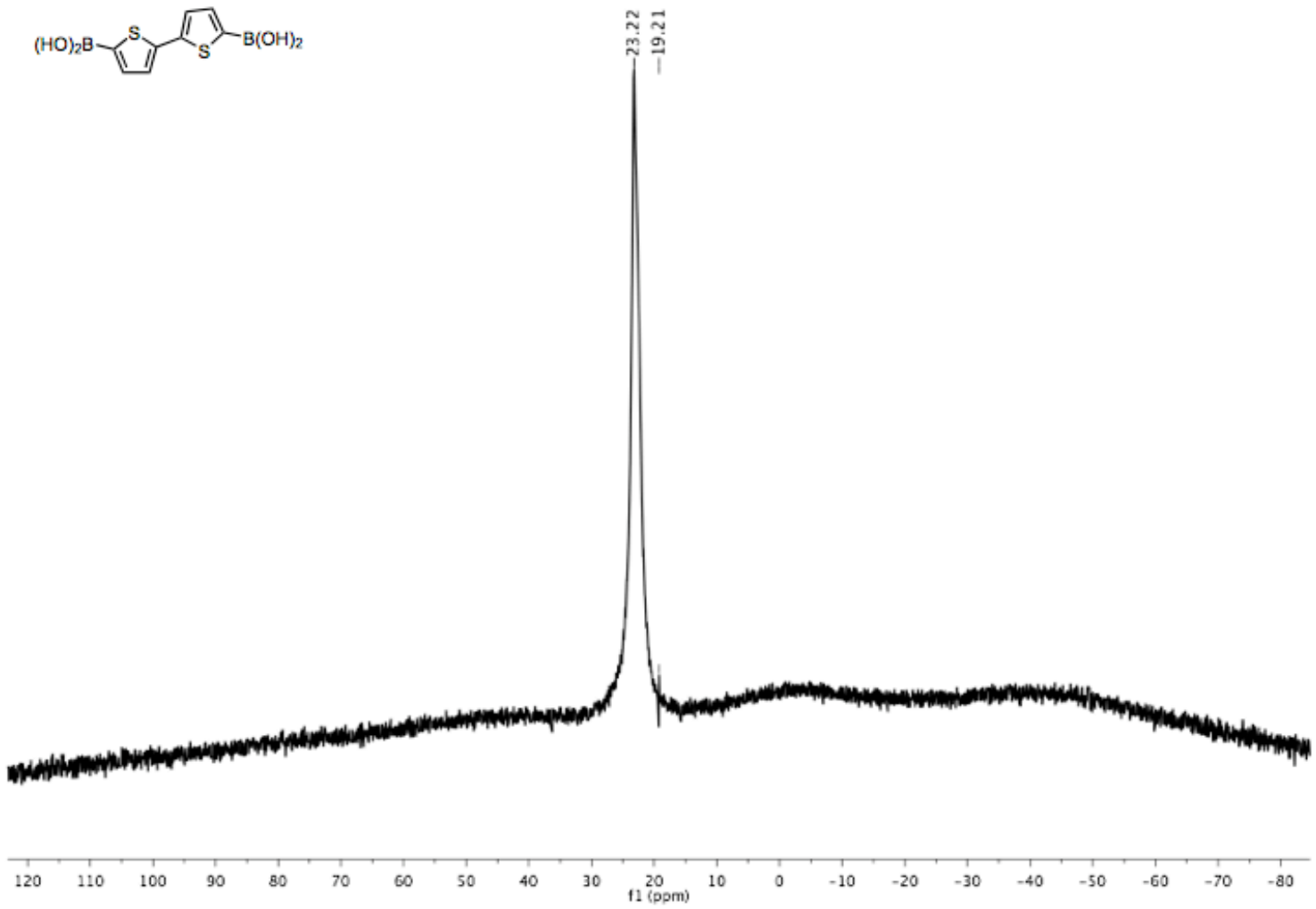

Appendix Figure 3.9. ^{11}B NMR of compound **3** in $CDCl_3$

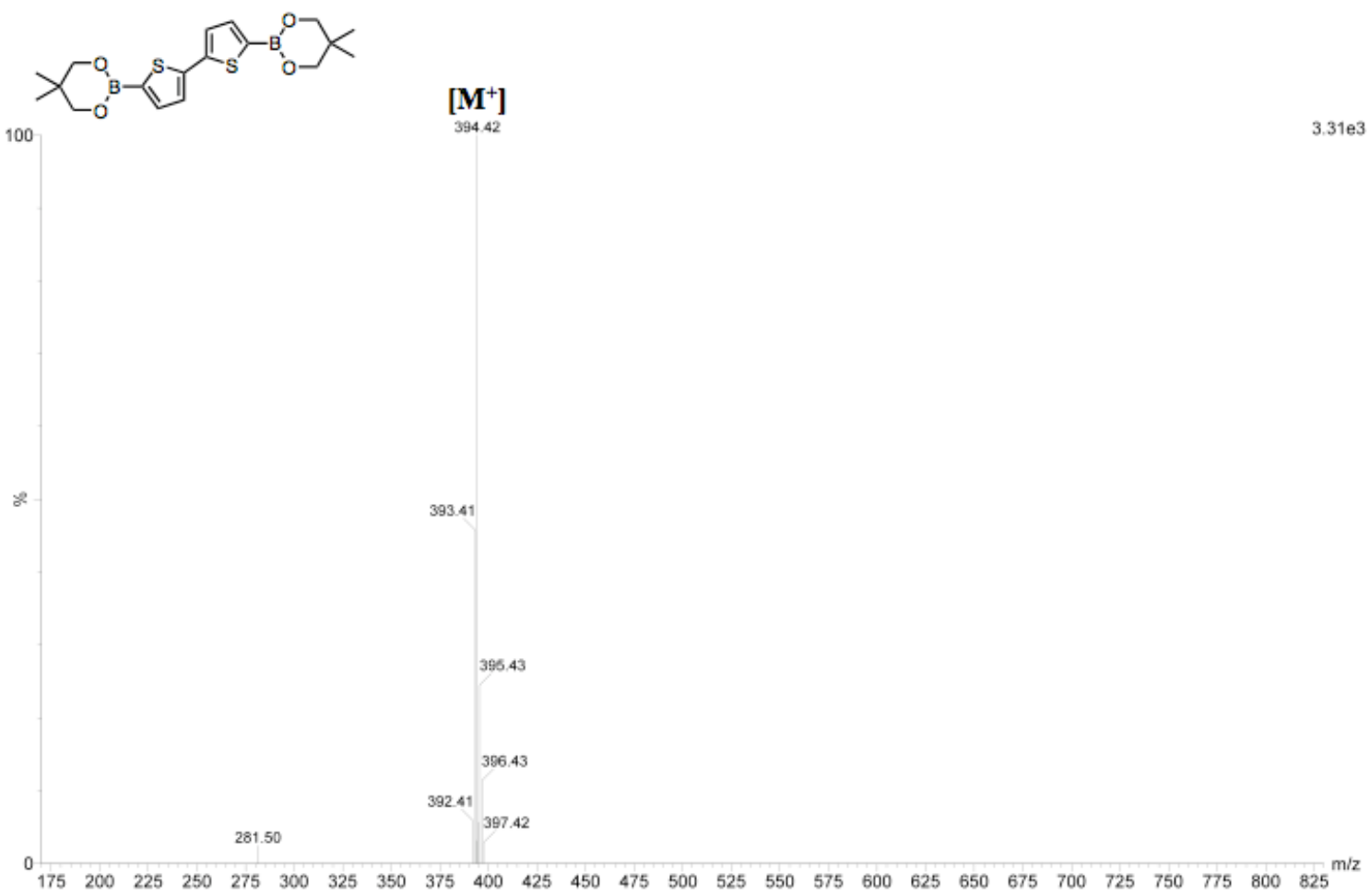

Appendix Figure 3.10. MALDI-TOF MS of compound **3**

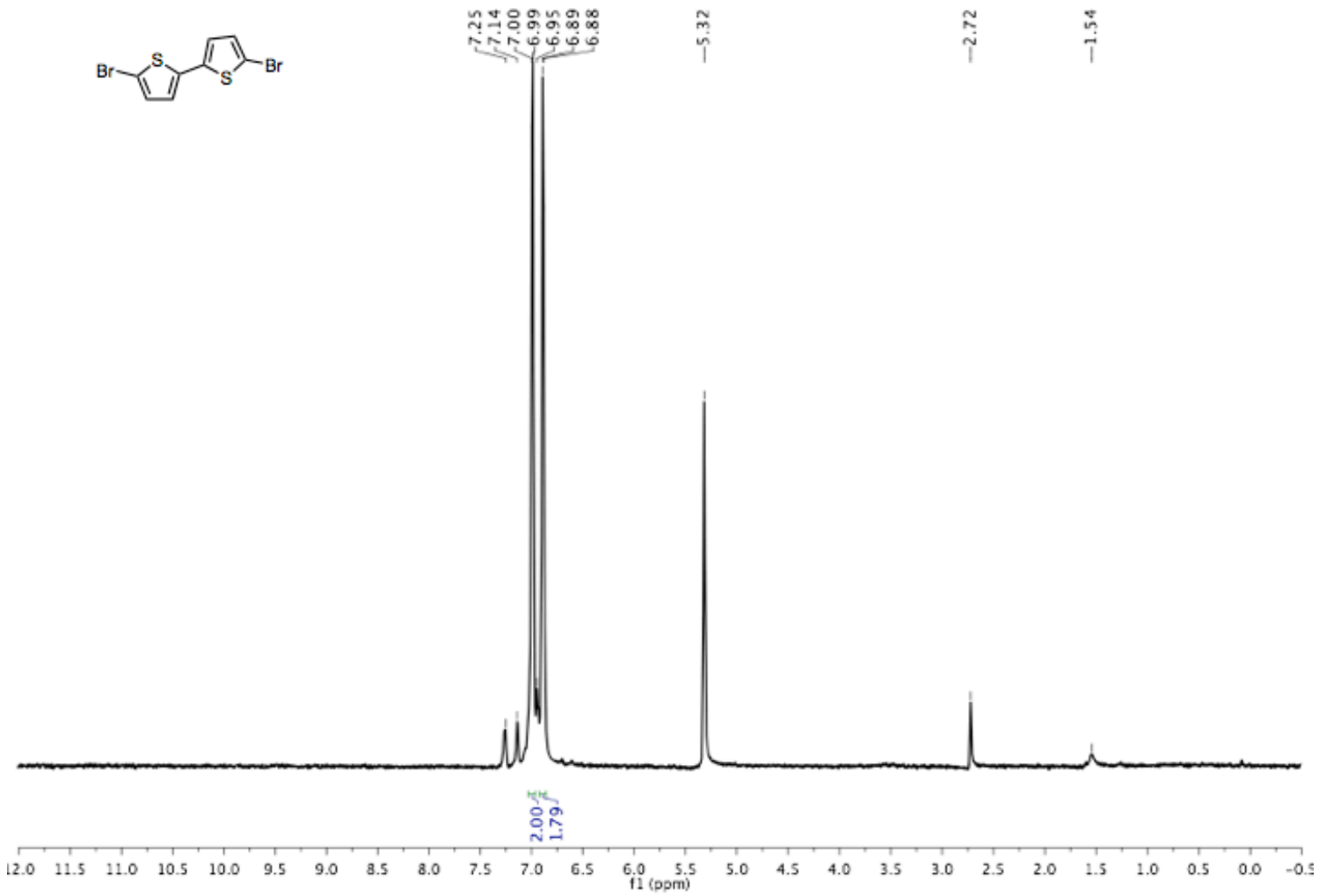

Appendix Figure 3.11. ^{1}H NMR of compound **4** in CD_2Cl_2

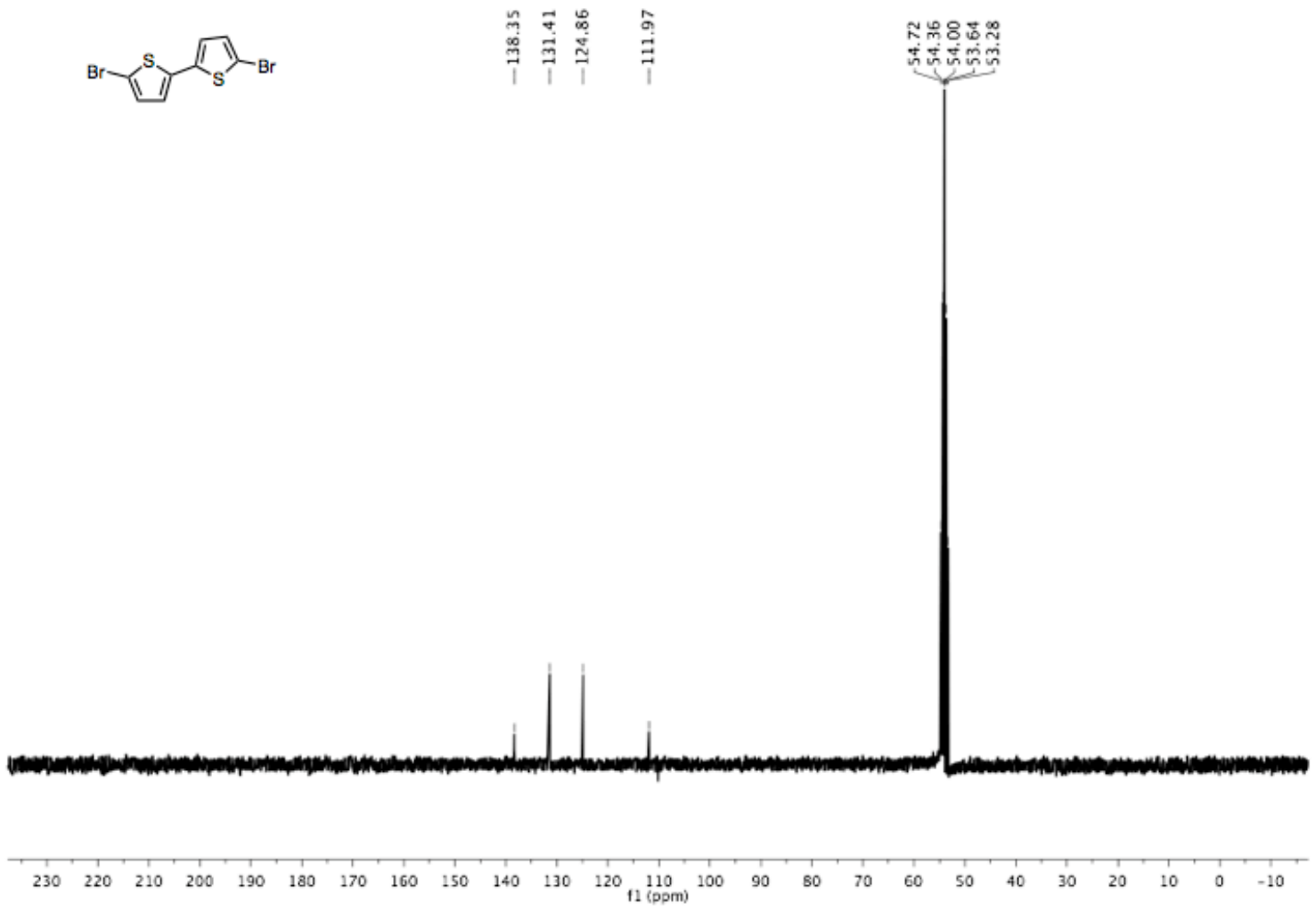

Appendix Figure 3.12. ^{13}C NMR of compound **4** in CD_2Cl_2

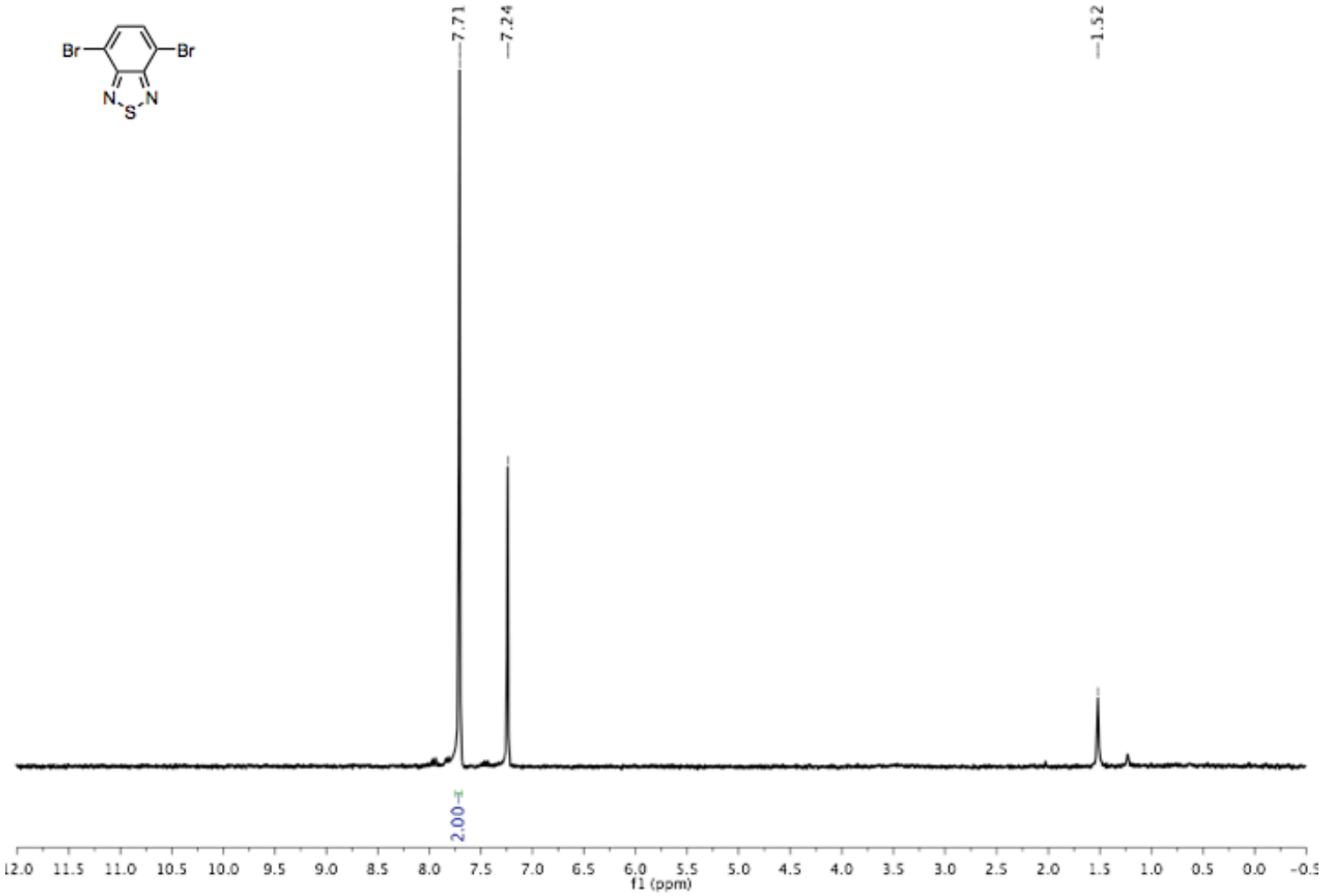

Appendix Figure 3.13. ^{1}H NMR of compound **5** in $CDCl_3$

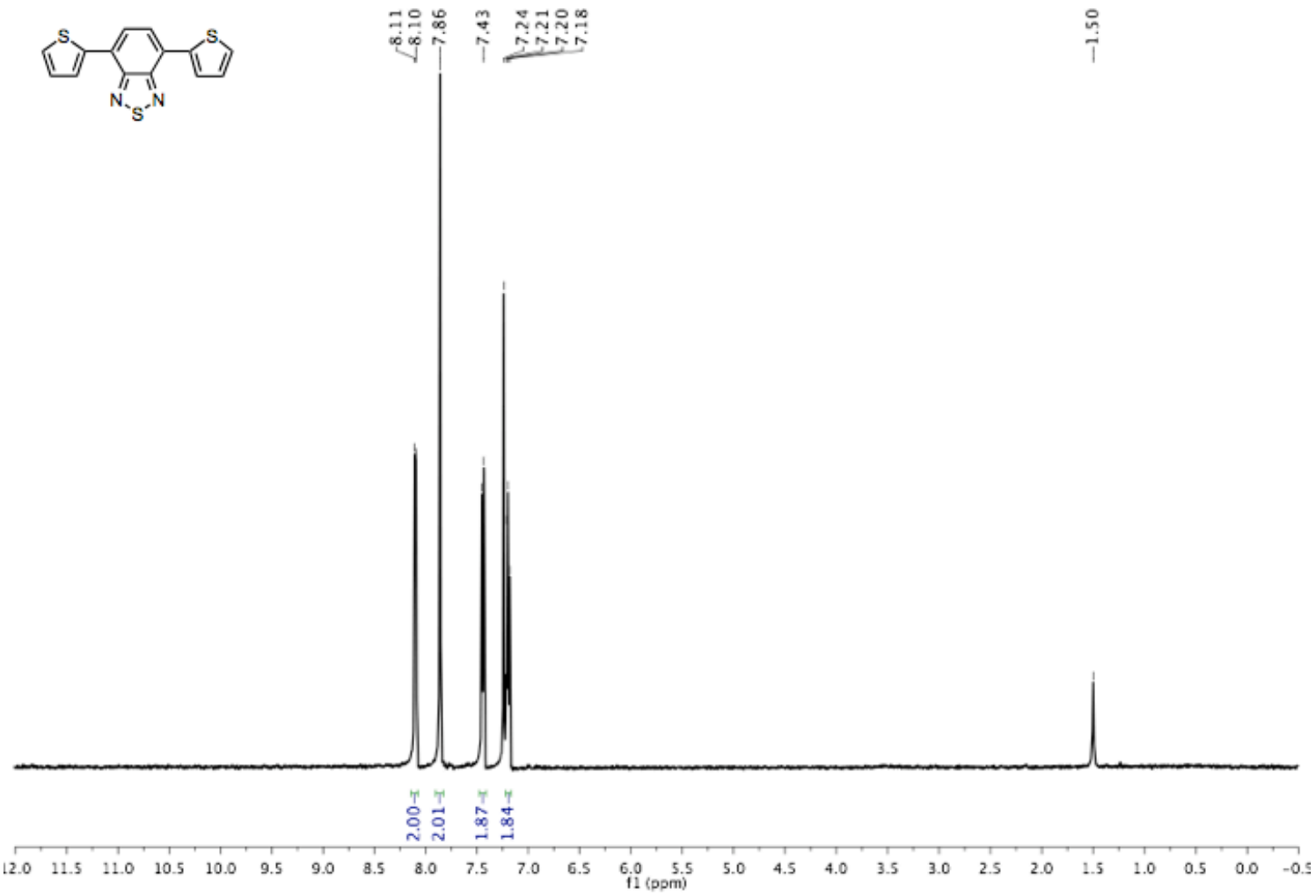

Appendix Figure 3.14. ^{1}H NMR of compound **6** in $CDCl_3$

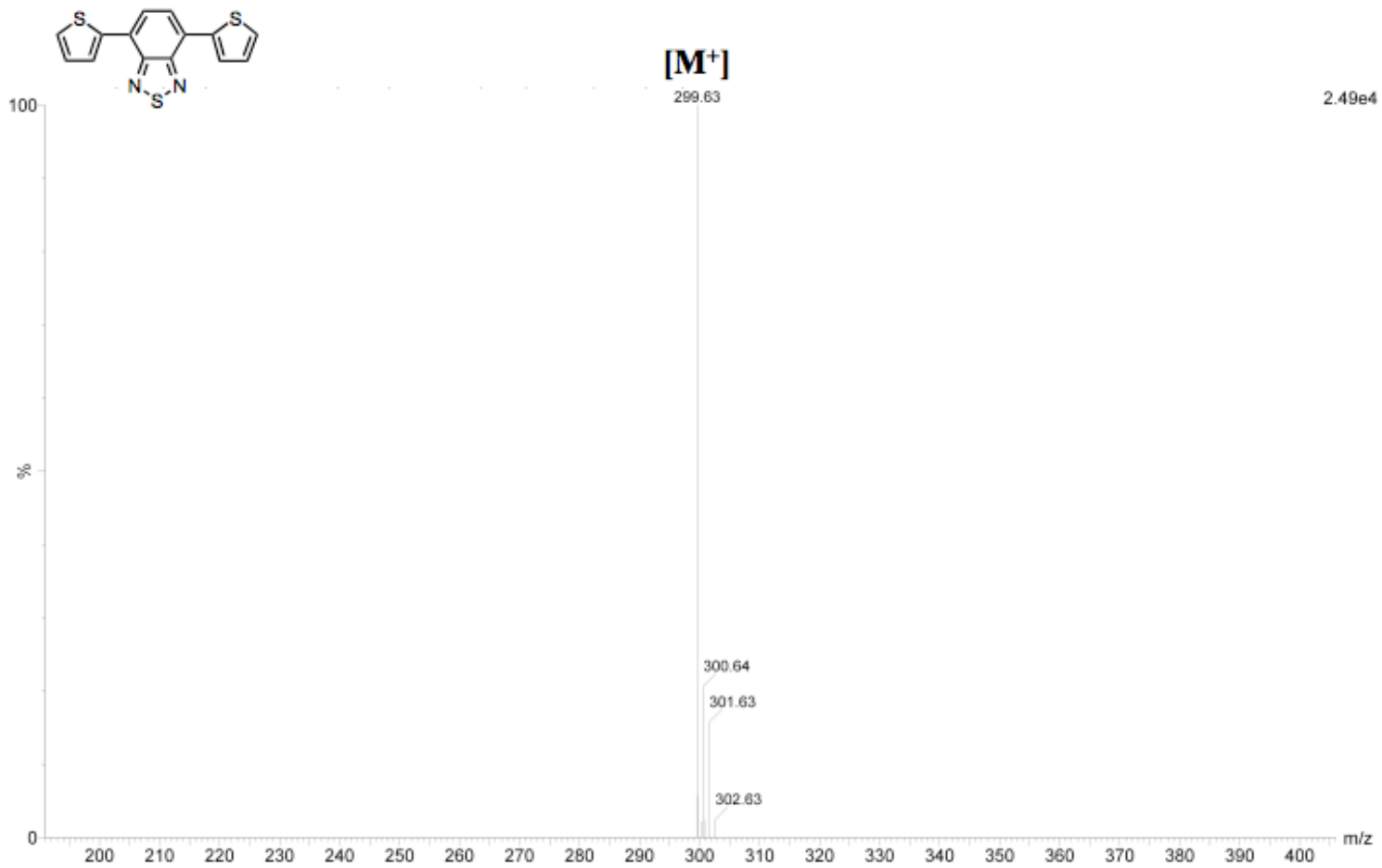

Appendix Figure 3.15. MALDI-TOF MS of compound **6**

REFERENCES

1. Dienes, Y.; Durben, S.; Kárpáti, T.; Neumann, T.; Englert, U.; Nyulászi, L.; Baumgartner, T. *Chem. Eur. J.* **2007**, *13*, 7487-7500.

2. Querner, C.; Benedetto, A.; Demadrille, R.; Rannou, P.; Reiss, P. *Chem. Mater.* **2006**, *18*, 4817-4826.

3. Gondo, S.; Goto, Y.; Era, M.; *Mol. Cryst. Liq. Cryst.* **2007**, *470*, 353-358.

4. Sakamoto, K.; Takashima, Y.; Yamaguchi, H.; Harada, A. *J. Org. Chem.* **2007**, *72*, 459-465.

5. Hicks, R.; Nodwell, M. *J. Am. Chem. Soc.* **2000**, *122*, 6746-6753.

6. Mishra, A.; Ma, C.; Bauerle, P. *Chem. Rev*. **2009**, *109*, 1141-1278.

7. Sirringhaus, H.; Tessler, N.; Friend, R. *Science*. **1998**, *280*, 1741-1745.

8. Takahashi, M.; Masui, K.; Sekiguchi, H.; Kobayashi, N.; Mori, A.; Funahashi, M.; Tamaoki, N. *J. Am. Chem. Soc.* **2006**, *128*, 10930-10933.

9. Rambo, B.; Lavigne, J. *Chem. Mater.* **2007**, *19*, 3732-3739.

10. Côté, A.; Benin, A.; Ockwig, N.; O'Keeffe, M.; Matzger, A.; Yaghi, O. *Scienc*e. **2005**, *310*, 1166-1170.

11. Knapp, D.; Gillis, E.; Burke, M. *J. Am. Chem. Soc.* **2009**, *13*, 6961-6963.

12. Longstaff, C.; Rose, M. *Org. Mass. Spectrom.* **1982**, *17*, 508-518.

13. Hall, D. *Boronic Acids: Preparations, Applications in Organic Synthesis and Medicine*. Weinheim: Wiley-VCH, **2005**.

14. Lightowler, S.; Hird, M. *Chem. Mater.* **2005**, *17*, 5538-5549.

15. Roncali, J. *Acc. Chem. Res.* **2009**, *42*, 1719-1730.

16. Neto, B.; Lopes, A.; Wüst, M.; Costa, V.; Ebeling, G.; Dupont, J. *Tet. Let*. **2005**, *46*, 6843-6846.

17. Cremer, J.; Osteritz-Mena, E.; Pschierer, N.; Müllen, K.; Bäurle, P. *Org. Biomol. Chem.* **2005**, *3*, 985-995.

18. Liang, F.; Lu, J.; Ding, J.; Movileanu, R.; Tao, Y. *Macromolecules*, **2009**, *42*, 6107-6114.